transmission rate, and HLA allele prevalence. Models would need to include factors such as the selection of compensatory mutations to slow reversion rates, and antiretroviral therapy access that would slow transmission rates.

HLA adaptation to certain $CD8^+$ T-cell responses may also alter currently established HLA associations with slow disease progression. Data here suggest that, whereas 25 years ago HLA-B*51 was protective in Japan[11,12], this is no longer the case (Supplementary Fig. 2). The apparent increase in I135X frequency in Japan over this time supports the notion that HLA-B*51 protection against HIV disease progression hinges on availability of the HLA-B*51-restricted TAFTIPSI response. However, whether this is the case remains unknown.

For HLA-B*27 and HLA-B*57, there is more clear-cut evidence that their association with HIV control depends on the Gag-specific epitopes presented and analysed here[4,7,13–15,18,19]. For each of the HLA-B*27- and HLA-B*57-associated Gag mutations studied, an *in vitro* fitness cost or *in vivo* reversion has been observed. A strong correlation between variant frequency and HLA prevalence even for rapidly reverting variants can be explained, either by mutant acquisition exceeding reversion rate (Fig. 4D), or by selection of compensatory mutations slowing or halting reversion altogether. The clearest example of the latter is the HLA-B*27-associated R264K mutation, 'corrected' by S173A[19]. Compensatory mutations are also well described for the HLA-B*57-associated Gag mutations[14,18]. These data suggest that the escape mutations in these HLA-B*27- and HLA-B*57-restricted epitopes are accumulating over time. Several studies have now demonstrated that transmission of viruses encoding escape mutants in the critical Gag epitopes to individuals expressing the relevant MHC class results in failure to control viraemia[2,21,22]. The accumulation at the population level of these escape mutations in HLA-B*27 and HLA-B*57 Gag epitopes is therefore likely to reduce the facility of these alleles to slow HIV disease progression.

The longer-term consequences of this process for immune control of HIV are unknown. Loss of currently immunodominant epitopes would promote subdominant $CD8^+$ T-cell responses, which can be more effective[23,24]. Also, the adapted virus provides new epitopes that can be presented, potentially with beneficial effects. In hepatitis C virus, for example, HLA-A*0301 holds a particular advantage, but only against the specific strain of virus responsible for the Irish outbreak[25]. In HIV, HLA-B*1801 is associated with high viraemia in C clade but not in B clade infection[10,11,26]; the opposite applies to HLA-B*5301.

Thus, the data presented here, showing evidence that the virus is adapting to $CD8^+$ T-cell responses, some of which may mediate the well-established associations (HLA-B*57, HLA-B*27 and HLA-B*51) with immune control of HIV, highlight the dynamic nature of the challenge for an HIV vaccine. Important questions to be addressed include the speed and extent of sequence change, particularly in Gag, the most effective target for $CD8^+$ T-cell responses[1,7,13,21]. The induction of broad Gag-specific $CD8^+$ T-cell responses may be a successful vaccine strategy, but such a vaccine will be most effective if tailored to the viral sequences prevailing, and thus may need to be modified periodically to keep pace with the evolving virus. Moreover, the strong associations between certain HLA class molecules, such as HLA-B*57, HLA-B*27 and HLA-B*51, and slow disease progression may decline as the epidemic continues, particularly where these HLA alleles are highly prevalent, and where HIV transmission rates are high.

METHODS SUMMARY

Overall 2,875 subjects were studied, from 9 previously established study cohorts. These cohorts comprised subjects from North America, the Caribbean, Europe, sub-Saharan Africa, Australasia and Asia. All subjects were antiretroviral-therapy-naive. Apart from the London acute cohort ($n = 142$), all cohorts comprised chronically infected subjects. The 14 variants studied are well-defined escape mutations within well-characterized $CD8^+$ T-cell epitopes, and included those persisting after transmission and likely to have little effect on viral fitness ($n = 5$), as well as those shown previously to reduce viral fitness ($n = 9$). Autologous HIV-1 sequences, and HLA class I types, were determined for all study subjects. The replicative capacity of I135X variants selected within the HLA-B*51-restricted epitope TAFTIPSI (RT 128–135) was assessed via *in vitro* competition assays and also via longitudinal follow-up of HLA-B*51-negative subjects infected acutely with I135X variants. Polymorphism frequency in the study cohorts was compared with prevalence of the relevant HLA molecule in the study cohort using a logistic regression model taking into account the different numbers of study subjects in each cohort. Demonstration of an HLA allele driving escape at Gag 146 in the Japanese cohort was undertaken first by identification of an association between HLA-B*4801 and A146P, subsequent definition of an HLA-B*4801-restricted $CD8^+$ T-cell response to a novel epitope Gag 138–147 (LI10), and finally demonstration that A146P reduced viral recognition by LI10-specific $CD8^+$ T cells.

Full Methods and any associated references are available in the online version of the paper at www.nature.com/nature.

Received 13 October; accepted 22 December 2008.
Published online 25 February 2009.

1. Goulder, P. J. R. & Watkins, D. I. Impact of MHC class I diversity on immune control of immunodeficiency virus replication. *Nature Rev. Immunol.* 8, 619–630 (2008).
2. Goulder, P. J. R. *et al.* Evolution and transmission of stable CTL escape mutations in HIV infection. *Nature* 412, 334–338 (2001).
3. Moore, C. B. *et al.* Evidence of HIV-1 adaptation to HLA-restricted immune responses at a population level. *Science* 296, 1439–1443 (2002).
4. Draenert, R. *et al.* Immune selection for altered antigen processing leads to cytotoxic T lymphocyte escape in chronic HIV-1 infection. *J. Exp. Med.* 199, 905–915 (2004).
5. Leslie, A. J. *et al.* Transmission and accumulation of CTL escape variants drive negative associations between HIV polymorphisms and HLA. *J. Exp. Med.* 201, 891–902 (2005).
6. Bhattacharya, T. *et al.* Founder effects in the assessment of HIV polymorphisms and HLA allele associations. *Science* 315, 1583–1586 (2007).
7. Matthews, P. *et al.* Central role of reverting mutations in HLA associations with viral setpoint. *J. Virol.* 82, 8548–8559 (2008).
8. Tomiyama, H. *et al.* Identification of multiple HIV-1 CTL epitopes presented by HLA-B*5101 molecules. *Hum. Immunol.* 60, 177–186 (1999).
9. Brumme, Z. *et al.* Human leukocyte antigen-specific polymorphisms in HIV-1 Gag and their association with viral load in chronic untreated infection. *AIDS* 22, 1277–1286 (2008).
10. Itoh, Y. *et al.* High throughput DNA tying of HLA-A, -B, -C, and -DRB1 loci by a PCR-SSOP-Luminex method in the Japanese population. *Immunogenetics* 57, 717–729 (2005).
11. Kaslow, R. A. *et al.* Influence of combinations of human major histocompatibility complex genes on the course of HIV-1 infection. *Nature Med.* 2, 405–411 (1996).
12. O'Brien, S. J., Gao, X. & Carrington, M. HLA and AIDS: a cautionary tale. *Trends Mol. Med.* 7, 379–381 (2001).
13. Kiepiela, P. *et al.* $CD8^+$ T-cell responses to different HIV proteins have discordant associations with viral load. *Nature Med.* 13, 46–53 (2007).
14. Leslie, A. J. *et al.* HIV evolution: CTL escape mutation and reversion after transmission. *Nature Med.* 10, 282–289 (2004).
15. Goulder, P. J. R. *et al.* Late escape from an immunodominant cytotoxic T-lymphocyte response associated with progression to AIDS. *Nature Med.* 3, 212–217 (1997).
16. Feeney, M. E. *et al.* Immune escape precedes breakthrough HIV-1 viremia and broadening of the CTL response in a HLA-B27-positive long-term nonprogressing child. *J. Virol.* 78, 8927–8930 (2004).
17. Martinez-Picado, J. *et al.* Fitness cost of escape mutations in p24 Gag in association with control of human immunodeficiency virus type 1. *J. Virol.* 80, 3617–3623 (2006).
18. Crawford, H. *et al.* Compensatory mutation partially restores fitness and delays reversion of escape mutation within the immunodominant HLA-B*5703-restricted Gag epitope in chronic human immunodeficiency virus type 1 infection. *J. Virol.* 81, 8346–8351 (2007).
19. Schneidewind, A. *et al.* Escape from a dominant Gag-specific CTL response in HLA-$B27^+$ subjects is associated with a dramatic reduction in HIV-1 replication. *J. Virol.* 81, 12382–12393 (2007).
20. Brumme, Z. *et al.* Marked epitope- and allele-specific differences in rates of mutation in human immunodeficiency type 1 (HIV-1) Gag, Pol, and Nef cytotoxic T-lymphocyte epitopes in acute/early HIV-1 infection. *J. Virol.* 82, 9216–9227 (2008).
21. Goepfert, P. *et al.* Transmission of Gag immune escape mutations is associated with reduced viral load in linked recipients. *J. Exp. Med.* 205, 1009–1017 (2008).
22. Seki, S. *et al.* Transmission of SIV carrying multiple cytotoxic T lymphocyte escape mutations with diminished replicative capacity can result in AIDS progression in Rhesus macaques. *J. Virol.* 82, 5093–5098 (2008).

23. Gallimore, A., Dumrese, T., Hengartner, H., Zinkernagel, R. M. & Rammensee, H. G. Protective immunity does not correlate with the hierarchy of virus-specific cytotoxic T cell responses to naturally processed peptides. *J. Exp. Med.* **187**, 1647–1657 (1998).
24. Holtappels, R. *et al.* Subdominant CD8 T-cell epitopes account for protection against cytomegalovirus independent of immunodomination. *J. Virol.* **82**, 5781–5796 (2008).
25. McKiernan, S. M. *et al.* Distinct MHC class I and II alleles are associated with hepatitis C viral clearance, originating from a single source. *Hepatology* **40**, 108–114 (2004).
26. Kiepiela, P. *et al.* Dominant influence of HLA-B in mediating the potential co-evolution of HIV and HLA. *Nature* **432**, 769–775 (2004).

Supplementary Information is linked to the online version of the paper at www.nature.com/nature.

Acknowledgements This work is funded by grants from the National Institutes of Health (RO1AI46995 (P.G.), 1 R01 AI067073 (B.D.W.), R01AI64060 (E.H.)), the Wellcome Trust (P.G., P.K.), the UK Medical Research Council (J.F., A.P. and P.M.), and the Mark and Lisa Schwartz Foundation, the Ministry of Health, Labour and Welfare (Health and Labour HIV/AIDS Research Grants 012), the NIHR Biomedical Research Centre Programme and the Ministry of Education, Science, Sports and Culture (number 18390141), Japan (M.T.). P.G. is an Elizabeth Glaser Pediatric AIDS Foundation Scientist; J.G.P. is a Marie Curie Fellow (contract number IEF-041811). The authors are also grateful to A. McLean and H. Fryer for discussions of the manuscript.

Author Contributions Y.K., K.P., J.F. and P. M. undertook much of the experimental work and data analysis, and contributed equally. M.T. and P.G. undertook much of the project conception, planning, supervision, analysis and writing of the manuscript, and contributed equally.

Author Information Accession numbers for newly determined viral sequences are included in Supplementary Information. Reprints and permissions information is available at www.nature.com/reprints. Correspondence and requests for materials should be addressed to P.G. (philip.goulder@paediatrics.ox.ac.uk).

Antiviral Research 82 (2009) 115–121

Contents lists available at ScienceDirect

Antiviral Research

journal homepage: www.elsevier.com/locate/antiviral

Clinical relevance of substitutions in the connection subdomain and RNase H domain of HIV-1 reverse transcriptase from a cohort of antiretroviral treatment-naïve patients

Atsuko Hachiya[a,b], Kazuki Shimane[c,d], Stefan G. Sarafianos[e], Eiichi N. Kodama[c,*,1], Yasuko Sakagami[c], Fujie Negishi[a], Hirokazu Koizumi[b], Hiroyuki Gatanaga[a,b], Masao Matsuoka[c], Masafumi Takiguchi[b], Shinichi Oka[a,b]

[a] AIDS Clinical Center, International Medical Center of Japan, Japan
[b] Center for AIDS Research, Kumamoto University, Japan
[c] Institute for Virus Research, Kyoto University, 53 Kawaramachi, Shogoin, Sakyo-ku, Kyoto 606-8507, Japan
[d] Graduate School of Biostudies, Kyoto University, Japan
[e] Christopher Bond Life Sciences Center, Department of Molecular Microbiology and Immunology, University of Missouri School of Medicine, Columbia, MO, USA

ARTICLE INFO

Article history:
Received 27 October 2008
Received in revised form 27 January 2009
Accepted 9 February 2009

Keywords:
HIV-1
Antiretroviral treatment-naïve patient
Resistant mutation
Connection subdomain
RNase H domain

ABSTRACT

Some mutations in the connection subdomain of the polymerase domain and in the RNase H domain of HIV-1 reverse transcriptase (RT) have been shown to contribute to resistance to RT inhibitors. However, the clinical relevance of such mutations is not well understood. To address this point we determined the prevalence of such mutations in a cohort of antiretroviral treatment-naïve patients ($n = 123$) and assessed whether these substitutions are associated with drug resistance *in vitro* and *in vivo*. We report here significant differences in the prevalence of substitutions among subtype B, and non-subtype B HIV isolates. Specifically, the E312Q, G333E, G335D, V365I, A371V and A376S substitutions were present in 2–6% of subtype B, whereas the G335D and A371V substitutions were commonly observed in 69% and 75% of non-B HIV-1 isolates. We observed a significant decline in the viral loads of patients that were infected with HIV-1 carrying these substitutions and were subsequently treated with triple drug regimens, even in the case where zidovudine (AZT) was included in such regimens. We show here that, generally, such single substitutions at the connection subdomain or RNase H domain have no influence on drug susceptibility *in vitro* by themselves. Instead, they generally enhance AZT resistance in the presence of excision-enhancing mutations (EEMs, also known as thymidine analogue-associated mutations, TAMs). However, N348I, A376S and Q509L did confer varying amounts of nevirapine resistance by themselves, even in the absence of EEMs. Our studies indicate that several connection subdomain and RNase H domain substitutions typically act as pre-therapy polymorphisms.

1. Introduction

The zidovudine (AZT)-resistance mutations reside at the DNA polymerase domain of HIV-1 reverse transcriptase (RT). They are associated either with (a) the exclusion mechanism that enhances discrimination at the point of AZT monophosphate (AZT-MP) incorporation through a set of mutations at codons A62, V75, F77, F116 and Q151 of the polymerase domain (Deval et al., 2002; Ueno and Mitsuya, 1997), or with (b) the excision mechanism that involves selective removal of AZT-MP after it has been incorporated by RT into the viral DNA (Boyer et al., 2001; Meyer et al., 1999). The excision mechanism is associated with mutations at the polymerase domain, including M41L, D67N, K70R, L210W, T215F/Y and K219E/Q (excision-containing mutations [EEMs] also known as thymidine analogue-associated mutations [TAMs]).

Certain mutations in the connection subdomain (CD; codons 322–440) of the polymerase domain or in the RNase H domain (codons 441–560) of HIV-1 RT have recently been shown to be associated with resistance to AZT (Brehm et al., 2007; Hachiya et al., 2008; Kemp et al., 1998; Nikolenko et al., 2007; Ntemgwa et al., 2007; Yap et al., 2007). In some cases it appears that mutations that affect AZT resistance have different phenotypes, depending on the presence or absence of other resistance mutations. For example, the polymorphism G333D/E does not confer drug resistance by itself, but has been reported to contribute significantly to dual AZT-lamivudine (3TC) resistance when combined with EEMs and M184V (Caride et al., 2000; Gallego et al., 2002; Kemp et al., 1998; Zelina

* Corresponding author. Tel.: +81 22 717 8220; fax: +81 22 717 8221.
E-mail address: ekodama@virus.kyoto-u.ac.jp (E.N. Kodama).
[1] Present address: Emerging Infectious Diseases, Tohoku University School of Medicine, 2-1 Seiryomachi, Aoba-ku, Sendai, 980-8575, Japan.

0166-3542/$ – see front matter © 2009 Elsevier B.V. All rights reserved.
doi:10.1016/j.antiviral.2009.02.189

et al., 2008). Similarly, A371V and Q509L, which were selected in the background of D67N and K70R by high concentrations of AZT *in vitro*, show strong resistance to AZT and weak cross-resistance to 3TC, abacavir (ABC) and tenofovir (TNF/PMPA) in the presence of EEMs (Brehm et al., 2007). Santos et al. (2008) also recently reported that the A360V and A371V mutations are frequently observed in AZT-treated patients. In contrast, one of the connection subdomain mutations, N348I, is associated with resistance to both nucleoside RT inhibitors (NRTIs) and non-nucleoside RT inhibitors (NNRTIs) and appears to be induced by regimens containing AZT, didanosine (ddI) and/or nevirapine (NVP) (Hachiya et al., 2008; Yap et al., 2007). Recently, it has been shown that the N348I mutation decreases the efficiency of RNase H cleavage and increases excision of AZT from AZT-terminated primer/templates, in the presence of the pyrophosphate donor ATP (Delviks-Frankenberry et al., 2008; Ehteshami et al., 2008; Yap et al., 2007). The decreased degradation of the RNA template by the diminished RNase H cleavage has been proposed to provide additional time for RT to excise AZT-MP and hence result in the observed increased AZT resistance (Delviks-Frankenberry et al., 2008; Ehteshami et al., 2008).

With the exception of N348I, the clinical relevance of these mutations remains to be clarified. A major obstacle to understanding the contribution of connection subdomain mutations to NRTI or NNRTI resistance has been the shortage of relevant sequencing data. This is because, until recently, the majority of commercially available genotypic and phenotypic assays have not been targeting this region of the enzyme. This is now changing, as more attention is being focused on such substitutions, following recent publications from us (Hachiya et al., 2008) and others (Yap et al., 2007) showing that at least one connection subdomain mutation, N348I, contributes to multi-class drug resistance. However, it has not yet been determined if the genotypic substitutions encountered in the connection subdomain of polymerase or in the RNase H domain of RT have any phenotypic impact or any effect on virologic response to subsequent therapies. Another important question is whether resistance testing now performed should include these mutations.

To ascertain whether some mutations at the connection subdomain or at the RNase H domain of RT that appear in the absence of known drug-resistance mutations of the polymerase domain are induced by reverse transcriptase inhibitor (RTI) treatment or are simply pre-existing polymorphisms, we determined the frequency of amino acid substitutions in antiretroviral treatment-naïve patients and assessed whether these substitutions at the reported sites (Brehm et al., 2007; Hachiya et al., 2008; Kemp et al., 1998; Nikolenko et al., 2007; Yap et al., 2007) can cause drug resistance by themselves. We also explored whether these substitutions may have any effect on the virologic response to subsequent therapies.

2. Materials and methods

2.1. Patients

A total of 123 clinical isolates were obtained from fresh plasma of treatment-naïve HIV-infected patients using MAGIC-5 cells as described previously (Hachiya et al., 2001). Written informed consent was obtained from each patient under approval by the Institutional Review Board of the International Medical Center of Japan (IMCJ-H13-80). The clinical course and antiretroviral therapies used were reviewed retrospectively.

2.2. Recombinant molecular clones

Recombinant molecular clones were generated as described previously (Hachiya et al., 2008). Briefly, the pBS-RT_{WT} contains almost entire RT coding sequence (amino acid position 14–560) containing silent mutations for cloning (restriction enzyme sites, Xma I and Xba I at 5′- and 3′-end of DNA fragment, respectively). After site directed mutagenesis, the mutated RT was ligated into the corresponding restriction enzyme site of the HIV infectious clone pNL101 (Hachiya et al., 2008; Shimura et al., 2008).

2.3. Genotypic and phenotypic assays

For the genotypic assay, viral RNA was extracted from the culture supernatant of clinical isolates, amplified by nested RT-PCR, and then directly sequenced as described previously (Hachiya et al., 2008). For subtype classification, the RT sequences were analyzed using the 'Genotyping' software (http://www.ncbi.nlm.nih.gov/projects/genotyping/formpage.cgi) which uses the BLAST algorithm. HIV-1 sequences in worldwide, treatment-naïve patients were obtained from the Stanford HIV Drug Resistance Database (http://hivdb.stanford.edu/index.html, accessed as late as 26 February 2008) and compared with our cohort. Prevalence of mutations at each codon were compared by the χ^2-test, or Fisher's exact test when the number of patients was smaller than 5.

For phenotypic assay, each clinical isolate was directly tested for drug susceptibility in triplicates, using the MAGIC-5 cell-based assay as described previously (Hachiya et al., 2001). Infectious viruses were obtained by transfection of 293T cells with individual HIV molecular clones containing the desired mutations that were introduced by site directed mutagenesis. Cells were subsequently harvested and examined with the MAGIC-5 cell based assay (Hachiya et al., 2001, 2008).

2.4. Measurements of HIV-1 viral load

To assess virologic outcome, HIV-1 viral loads in plasma were measured using the commercially available Amplicor HIV-1 Monitor Test (Version 1.5, Roche Diagnostics K.K., Basel, Switzerland). Mean change from 0 at weeks 4, 8, 12, 16, 20 and 24 were evaluated. The statistical significance of the longitudinal changes of HIV-1 viral load in plasma was assessed by the Mann–Whitney *U*-test.

2.5. Molecular modeling studies

The SYBYL and O programs were used to prepare molecular model of the complexes of HIV-1 RT in complex with RNA/DNA (Protein Data Bank code number 1HYS), and containing mutations A376S, N348I and Q509L that were introduced manually into the original 1HYS structure. After introduction of the mutations, the structure coordinates were optimized through 100 cycles of Coleman energy minimization protocol.

3. Results

3.1. Sequence analysis of RT region

We sequenced nearly the entire RT coding region (amino acid position 9–560) of 123 clinical isolates obtained from treatment-naïve patients. Among these isolates, six contained the known RTI-associated resistant mutations, D67N ($n=2$), K238S ($n=2$) (http://www.hiv.lanl.gov/content/index), V108I/K238S ($n=1$) and V106A/V108I/K238S ($n=1$), and thus were excluded from further analysis. The clinical isolates were obtained from six patients within 1 year of the diagnoses for HIV-1 infection. Prevalence of HIV-1 with drug-associated mutations in Japanese treatment-naïve patients is estimated at approximately 4% (Gatanaga et al., 2007) and in American and European patients at 8–27% (Descamps et al., 2005; Little et al., 2002; UK Collaborative Group on Monitoring the Transmission

of HIV Drug Resistance, 2001; Weinstock et al., 2004). Therefore, the prevalence in our cohort (4.8%) seems to be comparable or lower than in previous reports, suggesting that the six patients are treatment-naïve and newly infected from treated patients. The strong majority of the remaining samples in our cohort were of subtype B ($n = 101$ of a total of 117 isolates), while other subtypes were also identified (CRF01_AE, A, C and CRF12_BF, with12, 2, 1 and 1 isolates, respectively).

Substitutions at the connection subdomain and RNase H domain observed in this cohort and in previous reports (Brehm et al., 2007; Hachiya et al., 2008; Kemp et al., 1998; Nikolenko et al., 2007; Yap et al., 2007) are shown in Table 1. In the treatment-naïve patients of our cohort that were infected with subtype B ($n = 101$), the frequencies of all mutations associated with AZT-resistance (Brehm et al., 2007; Hachiya et al., 2008; Kemp et al., 1998; Nikolenko et al., 2007; Yap et al., 2007) were comparable to those (treatment-naïve) deposited in the Stanford HIV Drug Resistance Database, except for the A360T mutation. The G335D and A371V substitutions were more prevalent in the non-B, rather than in the B isolates of our cohort. Moreover, the G335D/A371V combination was observed in 9 (56.3%) of the non-B isolates. Other polymorphisms, including E312A/D/N/T, G335E/N/S, A360S/T, A371T, A376T/V and Q509H, were widely observed in all subtypes in our cohort as well as in the Stanford HIV Drug Resistance Database. None of the clinical isolates of our cohort had the G333D, G335C, N348I, A360I/V, and Q509L mutations.

3.2. Phenotypic assay for clinical isolates

Phenotypically, all clinical isolates showed little resistance to tested drugs (Table 1). Isolates with the V365I substitution ($n = 4$ in subtype B) showed slightly reduced susceptibility to 3TC (2.3-fold). However, V365I may not be clinically relevant, since generally at least 3-fold resistance is required for assigning 3TC resistance *in vivo* (Parkin et al., 2004; Rhee et al., 2006). Furthermore, the prevalence of V365I in treated and untreated patients in the Stanford HIV Drug Resistance Database is comparable (3.7% and 3.6%, respectively). Notably, clinical isolates from treatment-naïve patients from our cohort with HIV carrying the E312N, G335E/N or A376V substitutions displayed rather enhanced susceptibility (over five-fold) to

Table 1
Drug susceptibilities of 117 clinical isolates obtained from *treatment-naïve patients.*

Amino acid substitutions	Frequency[a] % (n)		Median fold change in resistance[b]			
	Subtype B ($n = 101$)	Non-B ($n = 16$)	AZT	3TC	NVP	EFV
E312	84.1 (85)	18.8 (3)	1.2	1.3	1	1.1
Q[c]	**3 (3)**	**0**	**1.3**	**1.4**	**1.2**	**1.1**
A	6.9 (7)	0	1.1	1.1	1.3	1
D	1 (1)	6.3 (1)	1.7	1.2	1.7	1.1
N	0	6.3 (1)	0.1	1.3	0.2	1.2
T	5 (5)	68.8 (11)[d]	0.8	1	1.1	1.1
G333	94.1 (95)	100 (16)	1.1	1.3	1.1	1.1
D[c]	**0**	**0**	–	–	–	–
E[c]	**5.9 (6)**	**0**	**1.4**	**1.5**	**1**	**1.4**
G335	95 (96)	25 (4)	1.2	1.4	1	1.1
C[c]	**0**	**0**	–	–	–	–
D[c]	**2 (2)**	**68.8 (11)[d]**	**0.7**	**0.9**	**1.1**	**1.1**
E	0	6.3 (1)	0.3	0.06	0.2	0.5
N	1 (1)	0	0.2	0.2	0.8	1.5
S	2 (2)	0	0.6	0.9	1.3	1.4
N348	100 (101)	100 (16)	1.1	1.3	1	1.1
I[c,e]	**0**	**0**	–	–	–	–
A360	79.2 (80)	87.5 (14)	1.1	1.3	1.1	1.1
I[c]	**0**	**0**	–	–	–	–
V[c]	**0**	**0**	–	–	–	–
S	0	6.3 (1)	0.7	1.2	1.5	0.8
T	20.8 (21)[f]	6.3 (1)	0.9	1.4	1	1.2
V365	96 (97)	100 (16)	1.1	1.2	1	1.1
I[c]	**4 (4)**	**0**	**1**	**2.3**	**1.7**	**1.3**
A371	96 (97)	25 (4)	1.2	1.3	1.1	1.1
V[c]	**3 (3)**	**75 (12)[d]**	**0.7**	**0.9**	**0.9**	**1.1**
T	1 (1)	0	0.5	1.3	0.7	0.7
A376	92.1 (93)	75 (12)	1.1	1.3	1	1.1
S[c]	**3 (3)**	**6.3 (1)**	**1.3**	**0.9**	**1**	**0.6**
T	5 (5)	12.5 (2)	1.2	1	1.4	1.2
V	0	6.3 (1)	0.1	1.3	0.2	1.2
Q509	98 (99)	100 (16)	1.1	1.3	1.1	1.1
L[c]	**0**	**0**	–	–	–	–
H	2 (2)	0	0.6	0.7	0.7	0.8

[a] Of 123 clinical isolates, six carried the known RTI-associated mutations and were excluded from this analysis.

[b] The drug susceptibility assay (Hachiya et al., 2001) was clinically accepted in Japan.

[c] Resistant mutations reported previously (Brehm et al., 2007; Delviks-Frankenberry et al., 2007, 2008; Hachiya et al., 2008; Kemp et al., 1998; Nikolenko et al., 2007; Ntemgwa et al., 2007; Santos et al., 2008; Yap et al., 2007) are indicated in bold. Greater than three-fold increase of EC_{50} compared to that of NL4-3 was defined as resistance.

[d] The prevalence of these substitutions (E312T, G335D and 371V) is significantly difference among treatment-naïve patients between subtype B and non-B isolates ($p < 0.0001$).

[e] N348I confers cross-resistance to NRTIs and NNRTIs (Hachiya et al., 2008; Yap et al., 2007).

[f] The prevalence of A360T is significantly higher in our cohort compared to the Stanford HIV Drug Resistance Database (8.7%, $p = 0.0021$).

Table 2
Drug susceptibilities of molecular HIV-1 clones.

Mutation	EC_{50}, μM (fold increase)[a]				
	NRTI			NNRTI	
	AZT	3TC	TNF[b]	NVP	EFV
WT	0.026 ± 0.009	0.42 ± 0.04	6.2 ± 1.5	0.023 ± 0.01	0.0012 ± 0.0001
E312Q	0.037 ± 0.006 (1.4)	0.36 ± 0.05 (0.9)	4.1 ± 1.4 (0.7)	0.056 ± 0.007 (2.4)	0.0009 ± 0.0002 (0.8)
G333D	0.04 ± 0.01 (1.5)	0.28 ± 0.1 (0.7)	4.5 ± 1.8 (0.7)	0.055 ± 0.01 (2.4)	0.0017 ± 0.0003 (1.4)
G335C	0.04 ± 0.02 (1.5)	0.45 ± 0.1 (1.1)	7.7 ± 1.1 (1.2)	0.065 ± 0.02 (2.8)	0.0007 ± 0.00009 (0.6)
N348I	0.14 ± **0.01 (5.4)**	0.56 ± 0.07 (1.3)	8.8 ± 1.9 (1.4)	0.24 ± **0.04 (10)**	0.0032 ± 0.0005 (2.7)
A360I	0.037 ± 0.01 (1.4)	0.35 ± 0.1 (0.8)	7.1 ± 2.1 (1.1)	0.038 ± 0.01 (1.7)	0.0009 ± 0.00008 (0.8)
A360V	0.03 ± 0.002 (1.2)	0.28 ± 0.09 (0.7)	5.7 ± 2.3 (0.9)	0.051 ± 0.01 (2.2)	0.0016 ± 0.0006 (1.3)
V365I	0.045 ± 0.008 (1.7)	0.27 ± 0.06 (0.6)	6.1 ± 2.0 (1)	0.066 ± 0.02 (2.9)	0.0013 ± 0.0002 (1.1)
A376S	0.053 ± 0.02 (2)	0.3 ± 0.03 (0.7)	5.9 ± 1.6 (1)	0.084 ± **0.02 (3.7)**	0.0022 ± 0.0004 (1.8)
Q509L	0.072 ± 0.02 (2.8)	0.45 ± 0.1 (1.1)	8.1 ± 2.7 (1.3)	0.21 ± **0.06 (9.1)**	0.0032 ± 0.0009 (2.7)

[a] Data means ± standard deviations from at least three independent experiments. The relative increase in the EC_{50} value compared with that in HIV-1_{WT} is given in parentheses. Bold indicates an increase in EC_{50} value greater than three-fold.

[b] TNF (PMPA) [(*R*)-9-(2-phosphonomethoxypropyl) adenine or tenofovir] is the active nucleotide of the clinical prodrug tenofovir disoproxil fumarate.

AZT and NVP, AZT, 3TC and NVP, and AZT and NVP, respectively (Table 1). In our cohort, in the absence of EEM mutations, A371V had no significant effect on drug resistance (Table 1). However, other studies have shown that combined with EEMs, A371V can confer strong resistance to AZT and A371V has also been recently reported to be associated with weak cross-resistance to 3TC, TNF/PMPA and ABC (Brehm et al., 2007). In our cohort, ABC inhibits efficiently the clinical isolates that contain the A371V substitution in the absence of EEMs ($n = 13$) either in a subtype B, or non-B background (median fold increase was 0.9-fold, data not shown). Further, the combination of A371V and G335D commonly observed in non-B isolates also showed no resistance to AZT, 3TC or ABC (0.7-, 1.0- and 1.1-fold increase in susceptibility as compared to wild-type HIV, respectively). These results demonstrate that none of the above substitutions that were observed in clinical isolates confer any significant resistance to NRTIs or NNRTIs in the absence of EEMs.

3.3. Phenotypic assay for molecular clones

To further expand our understanding of the role of substitutions in these RT regions on drug resistance we also prepared HIV-1 recombinant viruses with related mutations that have been reported previously in similar drug resistance studies (Brehm et al., 2007; Hachiya et al., 2008; Kemp et al., 1998; Nikolenko et al., 2007; Yap et al., 2007). The results shown in Table 2 confirm that in the absence of NRTI or NNRTI resistance mutations, most substitutions in the connection subdomain and RNase H domain (with the exception of N348I, A376S and Q509L) show no significant resistance to AZT, 3TC, TNF/PMPA, NVP or efavirenz (EFV) (less than three-fold), suggesting that these mutations act as secondary mutations and may enhance resistance that is caused by primary mutations and/or may somehow improve replication kinetics impaired by the primary mutations. Q509L, which has been reported to enhance

Table 3
Profiles of patients infected with HIV carrying connection subdomain substitutions, and initial therapies used in patient treatments.

Parameter	Combination for treatment-naïve patients infected HIV-1			
	With substitutions		Without substitutions	
	With AZT ($n = 8$)	Without AZT ($n = 13$)	With AZT ($n = 16$)	Without AZT ($n = 24$)
Male, *n* (%)	5(63)	10(77)	15(94)	23(96)
Median age (range)	37(27–60)	41(27–54)	36(24–55)	38(26–59)
Median baseline viral load, $\log_{10}$ copies/ml (range)	5.0(3.0–6.0)	5.0(4.2–5.8)	5.0(4.1–6.4)	5.2(4.2–6.3)
Median baseline CD4 cell count, cell/μl (range)	217(3–549)	110(3–332)	225(9–613)	170(4–760)
Substitutions in the connection subdomain, *n* (%)[a]				
E312Q	–	3(23)	–	–
G333E	2(25)	2(15)	–	–
G335D	3(38)	6(46)	–	–
V365I	2(25)	–	–	–
A371V	2(25)	5(38)	–	–
A376S	1(13)[b]	2(15)	–	–
Initial therapy, *n* (%)				
Zidovudine	8(100)	–	16(100)	–
Lamivudine	4(50)	11(85)	12(75)	24(100)
Stavudine	–	11(85)	–	20(83)
Didanosine	4(50)	–	4(25)	–
Abacavir	1(13)	1(8)	1(6)	3(13)
Tenofovir	–	1(8)	–	1(4)
Emtricitabine	–	1(8)	–	–
Nevirapine	–	–	–	3(13)
Efavirenz	2(25)	3(23)	9(56)	9(38)
One protease inhibitor (PI)	3(38)	7(54)	5(31)	7(29)
Dual-boosted PI	1(13)	2(15)	1(6)	5(21)

[a] E312Q, G333E, G335D, V365I, A371V and V376S were reported to be AZT-resistant mutations (Brehm et al., 2007; Kemp et al., 1998; Nikolenko et al., 2007).

[b] In this case, the viral load did not fall below the limits of detection.

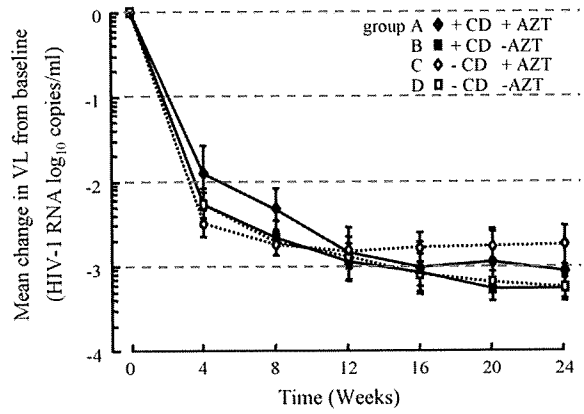

Fig. 1. Virological response up to 24 weeks after initiation of combination therapy. Mean (±standard error of the mean; S.E.M.) changes in plasma viral load (VL) were measured by Amplicor HIV-1 Monitor Test (Version 1.5, Roche Diagnostics K.K., Basel, Switzerland) from 0 to 24 weeks. Treatment-naive patients that were subsequently treated with combination therapy regimens are classified into four groups: patients that were infected with HIV-1 containing connection subdomain (CD) mutations and that subsequently received either combination therapy with AZT ($n = 8$, closed diamonds, group A) or without AZT ($n = 13$, closed squares, group B) and patients who were infected with HIV-1 with none of connection subdomain substitutions, and who subsequently received combination therapy with either AZT ($n = 16$, open diamonds with broken line, group C) or without AZT ($n = 24$, open squares with broken line, group D).

cross resistance to NRTIs in the presence of EEMs (Brehm et al., 2007), conferred little resistance to at least AZT, 3TC and TNF/PMPA in this study. Unlike N348I that confers dual resistance to NRTIs and NNRTIs, A376S and Q509L provided only NVP resistance.

3.4. Virological response after initiation of combination therapy

To further assess whether the CD substitutions at baseline are one of predictive factors of virologic outcome, we examined clinical samples from the treatment-naïve patients who subsequently received combination therapy through measuring virus load in plasma from 0 to 24 weeks (Table 3 and Fig. 1). The treatment-naïve patients were classified in four groups: (A) patients who were infected by HIV-1 that carried one or two of the CD substitutions E312Q, G333E, G335D, V365I, A371V or A376S and who subsequently received combination therapy that contained AZT ($n = 8$); (B) patients who were infected by HIV-1 that carried the above CD substitutions and who subsequently received combination therapy that did not contain AZT ($n = 13$); (C) patients who were infected by HIV-1 that did not carry any of the above CD substitutions and who subsequently received combination therapy containing AZT ($n = 16$); and (D) patients who were infected by HIV-1 that did not carry the above CD substitutions and who subsequently received combination therapy that did not contain AZT ($n = 24$). The mean change in viral load from baseline (week 0) to week 24 was from -2.76 to -3.28 $\log_{10}$ copies/ml among four groups. There were no significant differences in viral load changes up to 24 weeks among these groups (Fig. 1). Marginal viral suppression was observed in one patient who was infected by HIV-1 carrying A376S and who received combination therapy containing AZT. Any of the drug-associated resistant mutations were detected during the first 5 months of receiving combination therapy. However, HIV-1 protease mutations D30N and M36I that are responsible for resistance to NFV and HIV-1 RT D67N mutation that is responsible for AZT resistance eventually emerged. After switching to a new combination regimen (d4T/3TC/LPV), the viral load was successfully decreased. These results indicate that at least combination of two substitutions in the connection subdomain that are observed in treatment-naïve patients do not affect the virologic response of the ensuing combination therapy. Instead, they merely act as polymorphisms among the treatment-naïve patients.

4. Discussion

According to the crystal structure of HIV-1 RT in complex with RNA/DNA, some amino acids in the connection subdomain may affect binding to the RNA/DNA substrate (Sarafianos et al., 2001). It has been proposed that mutations at the connection subdomain may alter the binding affinity for nucleic acid at the connection subdomain and lead to enhanced resistance to AZT when combined with EEMs. This is thought to happen through a decrease in template RNA degradation which in turn provides additional time for RT to excise AZT-MP from the AZT-terminated template-primer$_{AZT\text{-}MP}$, thus causing resistance to AZT (Delviks-Frankenberry et al., 2007; Nikolenko et al., 2005, 2007). In our cohort, as well as in the Stanford HIV Drug Resistance Database, we observed a considerable number of treatment-naïve clinical samples containing substitutions (E312Q, G333E, G335D, V365I, A371V and A376S) that have been previously associated with AZT resistance. Our phenotypic studies with clinical isolates carrying mutations located in the connection subdomain of the polymerase or in the RNase H domain of RT revealed that in the absence of other known NRTI or NNRTI resistance mutations they do not cause by themselves significant resistance to the tested RTIs. Additionally, results from our cohort establish that the presence of G333E, G335D, V365I or A371V among treatment-naïve patients does not play any significant role in the virologic response after initiation of therapies that may, or may not, include AZT. We identified 25 isolates that have been deposited before 1986, prior to clinical trails for AZT in the Los Alamos HIV Sequence Database (http://www.hiv.lanl.gov/content/index). Some of these isolates also contained E312V, V365I, A376S/T/P, indicating that at least these substitutions are polymorphisms that preceded any antiviral therapy.

None of the isolates in our cohort had the H539N or H549N substitutions which have been proposed to be associated with resistance to NRTIs due to decreasing the frequency of RT template-switching and the level of RNase H activity (Nikolenko et al., 2004; Roquebert and Marcelin, 2008). Furthermore, the G333D, G335C, N348I, A360I/V and Q509L substitutions were not observed in our cohort, and were also rarely observed among treatment-naïve patients (less than 1%) in the Stanford HIV Drug Resistance Database. Their increased incidence among NRTI-treated patients as compared to untreated patients (>3-fold, >40-fold and >12-fold increases for G333C, N348I, and A360V respectively [http://hivdb.stanford.edu/cgi-bin/RTPosMutSummary.cgi]) and in the case of Q509L reported by others (Brehm et al., 2007; Roquebert et al., 2007) suggests that they are associated with AZT resistance. However, site directed mutagenesis studies showed that G333D (Kemp et al., 1998), G335C (Nikolenko et al., 2007), A360I/V (Nikolenko et al., 2007) and Q509L (Brehm et al., 2007) did not confer significant AZT resistance in the absence of other AZT resistance mutations. At present, only N348I has been shown to be involved in resistance to multiple RTIs (Hachiya et al., 2008; Yap et al., 2007). HIV with a serine at codon 376 also exhibits some NVP resistance in the absence of other mutations (Table 2). However, clinical isolates harboring different residues at position 376 exhibited no significant changes in their drug susceptibilities (Table 1). This discrepancy may arise from strain-specific polymorphisms that are present in the clinical isolates or the reference virus used in this study that may influence NVP susceptibility positively or negatively, respectively. In fact, we observe several polymorphisms in the majority of these isolates and it is possible that they somehow affect drug resistance. For instance, V118I has been identified in 2% of treatment-naïve patients as one of strain-specific polymorphisms, but more frequently observed in RTI-treated patients

(Delaugerre et al., 2001). Although this mutation by itself confers no resistance, it has been reported to contribute to hypersusceptibility to NNRTI (Clark et al., 2006) as well as resistance to NRTI in the presence of E44A/D and/or EEMs (Romano et al., 2002). Therefore, it is possible that polymorphisms present in our clinical isolates may also affect drug-susceptibility leading to minor discrepancies with the results obtained with recombinant virus.

In this study, the reference clone has an A376T polymorphism that is observed in a wide range of subtypes. Therefore, it is unlikely that A376T affects NVP susceptibility. Q509L confers moderate (~9-fold) resistance to NVP (Table 2). Although Q509L was not observed in our cohort, this mutation was found in the pretreated patients of another survey ($n = 118$) (Roquebert et al., 2007). These results indicate that introduction of Q509L may alter virologic responses, especially for NVP, although so far the clinical relevance and virological response of Q509L among the antiretroviral-experienced patients remains to be elucidated by further experiments.

Analysis of the crystal structure of RT bound to RNA/DNA showed that residues 376 (of the p66 subunit) and 509 are located relatively close to the nucleic-acid binding cleft of RT, and residue 348 of the p66 subunit is located close to the hinge region of the thumb subdomain and to the NNRTI-binding pocket (Fig. 2). Recently, Abbondanzieri et al. demonstrated that binding of nevirapine to RT causes conformational changes to the enzyme, allowing it to somehow relax the grip on nucleic-acid substrate (Abbondanzieri et al., 2008; Arnold and Sarafianos, 2008). NVP acts as a rapid-equilibrium inhibitor, not a tight-binding inhibitor as EFV (Maga et al., 2000; Motakis and Parniak, 2002), and it might be more sensitive to changes in the interaction between RT and the nucleic acid substrate. Thus, changes in the interactions of RT with nucleic-acid substrate could also influence the interaction balance between polymerase and RNase H activity and consequently might lead to RTI resistance. Nevertheless, additional biochemical and structural studies are warranted to define the exact mechanisms by which these mutations in the connection subdomain and RNase H domains confer NVP resistance.

Several studies have reported a correlation between two distinct types of EEMs in various HIV subtypes (Kantor et al., 2005; Montes et al., 2004; Novitsky et al., 2007). The Type I EEMs (M41L, L210W, T215Y and occasionally the D67N mutation) appear twice as frequently as Type II EEMs (D67N, K70R, T215F and K219Q mutation) in subtype B (Marcelin et al., 2004), whereas Type II EEMs are mostly observed in non-B isolates (Montes et al., 2004; Novitsky et al., 2007). Type II EEMs confer lower levels of AZT and TNF/PMPA resistance, as compared to Type I EEMs (Cozzi-Lepri et al., 2005; Miller et al., 2004). Addition of A371V to Type II EEM background conferred cross-resistance to AZT and tenofovir (Brehm et al., 2007). A371V was observed in the majority of non-B isolates in our cohort (75%) and the Stanford HIV Drug Resistance Database (96% in CRF01_AE). Therefore, it is possible that in the background of non-B isolates, the majority of which contains drug resistance associated connection subdomain mutations, smaller number of EEMs, especially Type II EEMs, might be preferentially selected for AZT and TNF/PMPA resistance. In the absence of EEMs, mutations at the connection subdomain of non-subtype B HIV, such as E312N, G335E or A376V, appear to act as simple polymorphisms, because they either maintain or enhance drug susceptibility in non-subtypes B HIV (Table 1). However, the A376S polymorphism in samples of treatment-naive patients or in a recombinant virus used in this study conferred mild NVP resistance (Table 2). These mutations were stable even in the absence of any drug treatment, suggesting that viral fitness of these variants is likely to be comparable to wild type non-subtype B HIV.

In this study we report the prevalence of amino acid substitutions in the connection subdomain of the polymerase domain and in the RNase H domain of RT in a cohort of treatment-naïve patients. We also determined the phenotypic susceptibility of these mutants to various RTIs. Our results support the hypothesis that the substitutions observed among treatment-naïve patients have little impact on therapeutic outcome by themselves in the absence of AZT-associated mutations, although certain substitutions, such as N348I, A376S, and Q509L, are involved in drug resistance even by themselves. These results may help improve existing interpretation algorithms and analysis of drug resistance mutations.

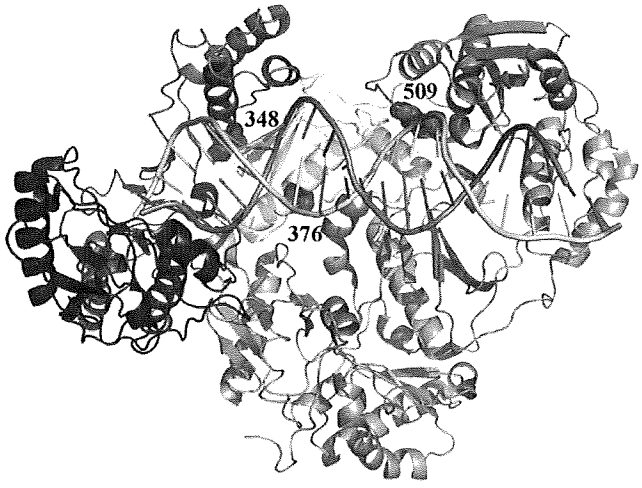

Fig. 2. Structure of HIV-1 RT in complex with RNA/DNA. The fingers, palm, thumb, connection subdomains, and RNase H domain of the p66 subunit colored in blue, red, green, yellow and orange, respectively. The p51 subunit is shown in dark yellow. Residue 348 of the p66 subunit is shown as pink Van der Waals spheres, and located proximally to the hinge region of the thumb subdomain and to the NNRTI binding pocket. Residues 376 and 509 of the p66 subunit are also shown, and are located proximally to the nucleic acid binding cleft.

Acknowledgments

This work was supported by a grant for the promotion of AIDS Research from the Ministry of Health, Labor and Welfare (AH, EK, MM, MT, and SO), a grant for Research for Health Sciences Focusing on Drug Innovation from The Japan Health Sciences Foundation (EK and MM), and by National Institute of Health (NIH) research grants AI076119, AI079801, and AI074389 to SGS. The authors thank Yukiko Takahashi for sample preparation.

References

Abbondanzieri, E.A., Bokinsky, G., Rausch, J.W., Zhang, J.X., Le Grice, S.F., Zhuang, X., 2008. Dynamic binding orientations direct activity of HIV reverse transcriptase. Nature 453, 184–189.

Arnold, E., Sarafianos, S.G., 2008. Molecular biology: an HIV secret uncovered. Nature 453, 169–170.

Boyer, P.L., Sarafianos, S.G., Arnold, E., Hughes, S.H., 2001. Selective excision of AZTMP by drug-resistant human immunodeficiency virus reverse transcriptase. J. Virol. 75, 4832–4842.

Brehm, J.H., Koontz, D., Meteer, J.D., Pathak, V., Sluis-Cremer, N., Mellors, J.W., 2007. Selection of mutations in the connection and RNase H domains of human immunodeficiency virus type 1 reverse transcriptase that increase resistance to 3′-azido-3′-dideoxythymidine. J. Virol. 81, 7852–7859.

Caride, E., Brindeiro, R., Hertogs, K., Larder, B., Dehertogh, P., Machado, E., de Sá, C.A., Eyer-Silva, W.A., Sion, F.S., Passioni, L.F., Menezes, J.A., Calazans, A.R., Tanuri, A., 2000. Drug-resistant reverse transcriptase genotyping and phenotyping of B and non-B subtypes (F and A) of human immunodeficiency virus type I found in Brazilian patients failing HAART. Virology 275, 107–115.

Clark, S.A., Shulman, N.S., Bosch, R.J., Mellors, J.W., 2006. Reverse transcriptase mutations 118I, 208Y, and 215Y cause HIV-1 hypersusceptibility to non-nucleoside reverse transcriptase inhibitors. AIDS 20, 981–984.

Cozzi-Lepri, A., Ruiz, L., Loveday, C., Phillips, A.N., Clotet, B., Reiss, P., Ledergerber, B., Holkmann, C., Staszewski, S., Lundgren, J.D., 2005. Thymidine analogue mutation profiles: factors associated with acquiring specific profiles and their impact on the virological response to therapy. Antivir. Ther. 10, 791–802.

Delaugerre, C., Mouroux, M., Yvon-Groussin, A., Simon, A., Angleraud, F., Huraux, J.M., Agut, H., Katlama, C., Calvez, V., 2001. Prevalence and conditions of selection of

E44D/A and V118I human immunodeficiency virus type 1 reverse transcriptase mutations in clinical practice. Antimicrob. Agents Chemother. 45, 946–948.
Delviks-Frankenberry, K.A., Nikolenko, G.N., Barr, R., Pathak, V.K., 2007. Mutations in human immunodeficiency virus type 1 RNase H primer grip enhance 3′-azido-3′-deoxythymidine resistance. J. Virol. 81, 6837–6845.
Delviks-Frankenberry, K.A., Nikolenko, G.N., Boyer, P.L., Hughes, S.H., Coffin, J.M., Jere, A., Pathak, V.K., 2008. HIV-1 reverse transcriptase connection subdomain mutations reduce template RNA degradation and enhance AZT excision. Proc. Natl. Acad. Sci. USA 105, 10943–10948.
Descamps, D., Chaix, M.L., André, P., Brodard, V., Cottalorda, J., Deveau, C., Harzic, M., Ingrand, D., Izopet, J., Kohli, E., Masquelier, B., Mouajjah, S., Palmer, P., Pellegrin, I., Plantier, J.C., Poggi, C., Rogez, S., Ruffault, A., Schneider, V., Signori-Schmück, A., Tamalet, C., Wirden, M., Rouzioux, C., Brun-Vezinet, F., Meyer, L., Costagliola, D., 2005. French national sentinel survey of antiretroviral drug resistance in patients with HIV-1 primary infection and in antiretroviral-naive chronically infected patients in 2001–2002. J. Acquir. Immune Defic. Syndr. 38, 545–552.
Deval, J., Selmi, B., Boretto, J., Egloff, M.P., Guerreiro, C., Sarfati, S., Canard, B., 2002. The molecular mechanism of multidrug resistance by the Q151M human immunodeficiency virus type 1 reverse transcriptase and its suppression using alpha-boranophosphate nucleotide analogues. J. Biol. Chem. 277, 42097–42104.
Ehteshami, M., Beilhartz, G.L., Scarth, B.J., Tchesnokov, E.P., McCormick, S., Wynhoven, B., Harrigan, P.R., Gotte, M., 2008. Connection domain mutations N348I and A360V in HIV-1 reverse transcriptase enhance resistance to 3′-azido-3′-deoxythymidine through both RNase H-dependent and H-independent mechanisms. J. Biol. Chem. 283, 22222–22232.
Gallego, O., Corral, A., de Mendoza, C., Rodés, B., Soriano, V., 2002. Prevalence of G333D/E in naive and pretreated HIV-infected patients. AIDS Res. Hum. Retroviruses 18, 857–860.
Gatanaga, H., Ibe, S., Matsuda, M., Yoshida, S., Asagi, T., Kondo, M., Sadamasu, K., Tsukada, H., Masakane, A., Mori, H., Takata, N., Minami, R., Tateyama, M., Koike, T., Itoh, T., Imai, M., Nagashima, M., Gejyo, F., Ueda, M., Hamaguchi, M., Kojima, Y., Shirasaka, T., Kimura, A., Yamamoto, M., Fujita, J., Oka, S., Sugiura, W., 2007. Drug-resistant HIV-1 prevalence in patients newly diagnosed with HIV/AIDS in Japan. Antiviral Res. 75, 75–82.
Hachiya, A., Aizawa-Matsuoka, S., Tanaka, M., Takahashi, Y., Ida, S., Gatanaga, H., Hirabayashi, Y., Kojima, A., Tatsumi, M., Oka, S., 2001. Rapid and simple phenotypic assay for drug susceptibility of human immunodeficiency virus type 1 using CCR5-expressing HeLa/CD4(+) cell clone 1-10 (MAGIC-5). Antimicrob. Agents Chemother. 45, 495–501.
Hachiya, A., Kodama, E.N., Sarafianos, S.G., Schuckmann, M.M., Sakagami, Y., Matsuoka, M., Takiguchi, M., Gatanaga, H., Oka, S., 2008. Amino acid mutation N348I in the connection subdomain of human immunodeficiency virus type 1 reverse transcriptase confers multiclass resistance to nucleoside and nonnucleoside reverse transcriptase inhibitors. J. Virol. 82, 3261–3270.
Kantor, R., Katzenstein, D.A., Efron, B., Carvalho, A.P., Wynhoven, B., Cane, P., Clarke, J., Sirivichayakul, S., Soares, M.A., Snoeck, J., Pillay, C., Rudich, H., Rodrigues, R., Holguin, A., Ariyoshi, K., Bouzas, M.B., Cahn, P., Sugiura, W., Soriano, V., Brigido, L.F., Grossman, Z., Morris, L., Vandamme, A.M., Tanuri, A., Phanuphak, P., Weber, J.N., Pillay, D., Harrigan, P.R., Camacho, R., Schapiro, J.M., Shafer, R.W., 2005. Impact of HIV-1 subtype and antiretroviral therapy on protease and reverse transcriptase genotype: results of a global collaboration. PLoS Med. 2, e112.
Kemp, S.D., Shi, C., Bloor, S., Harrigan, P.R., Mellors, J.W., Larder, B.A., 1998. A novel polymorphism at codon 333 of human immunodeficiency virus type 1 reverse transcriptase can facilitate dual resistance to zidovudine and L-2′, 3′-dideoxy-3′-thiacytidine. J. Virol. 72, 5093–5098.
Little, S.J., Holte, S., Routy, J.P., Daar, E.S., Markowitz, M., Collier, A.C., Koup, R.A., Mellors, J.W., Connick, E., Conway, B., Kilby, M., Wang, L., Whitcomb, J.M., Hellmann, N.S., Richman, D.D., 2002. Antiretroviral-drug resistance among patients recently infected with HIV. N. Engl. J. Med. 347, 385–394.
Maga, G., Ubiali, D., Salvetti, R., Pregnolato, M., Spadari, S., 2000. Selective interaction of the human immunodeficiency virus type 1 reverse transcriptase nonnucleoside inhibitor efavirenz and its thio-substituted analog with different enzyme-substrate complexes. Antimicrob. Agents Chemother. 44, 1186–1194.
Marcelin, A.G., Delaugerre, C., Wirden, M., Viegas, P., Simon, A., Katlama, C., Calvez, V., 2004. Thymidine analogue reverse transcriptase inhibitors resistance mutations profiles and association to other nucleoside reverse transcriptase inhibitors resistance mutations observed in the context of virological failure. J. Med. Virol. 72, 162–165.
Meyer, P.R., Matsuura, S.E., Mian, A.M., So, A.G., Scott, W.A., 1999. A mechanism of AZT resistance: an increase in nucleotide-dependent primer unblocking by mutant HIV-1 reverse transcriptase. Mol. Cell 4, 35–43.
Miller, M.D., Margot, N., Lu, B., Zhong, L., Chen, S.S., Cheng, A., Wulfsohn, M., 2004. Genotypic and phenotypic predictors of the magnitude of response to tenofovir disoproxil fumarate treatment in antiretroviral-experienced patients. J. Infect. Dis. 189, 837–846.
Montes, B., Vergne, L., Peeters, M., Reynes, J., Delaporte, E., Segondy, M., 2004. Comparison of drug resistance mutations and their interpretation in patients infected with non-B HIV-1 variants and matched patients infected with HIV-1 subtype B. J. Acquir. Immune Defic. Syndr. 35, 329–336.
Motakis, D., Parniak, M.A., 2002. A tight-binding mode of inhibition is essential for anti-human immunodeficiency virus type 1 virucidal activity of nonnucleoside reverse transcriptase inhibitors. Antimicrob. Agents Chemother. 46, 1851–1856.
Nikolenko, G.N., Delviks-Frankenberry, K.A., Palmer, S., Maldarelli, F., Fivash Jr., M.J., Coffin, J.M., Pathak, V.K., 2007. Mutations in the connection domain of HIV-1 reverse transcriptase increase 3′-azido-3′-deoxythymidine resistance. Proc. Natl. Acad. Sci. USA 104, 317–322.
Nikolenko, G.N., Palmer, S., Maldarelli, F., Mellors, J.W., Coffin, J.M., Pathak, V.K., 2005. Mechanism for nucleoside analog-mediated abrogation of HIV-1 replication: balance between RNase H activity and nucleotide excision. Proc. Natl. Acad. Sci. USA 102, 2093–2098.
Nikolenko, G.N., Svarovskaia, E.S., Delviks, K.A., Pathak, V.K., 2004. Antiretroviral drug resistance mutations in human immunodeficiency virus type 1 reverse transcriptase increase template-switching frequency. J. Virol. 78, 8761–8770.
Novitsky, V., Wester, C.W., DeGruttola, V., Bussmann, H., Gaseitsiwe, S., Thomas, A., Moyo, S., Musonda, R., Van Widenfelt, E., Marlink, R.G., Essex, M., 2007. The reverse transcriptase 67N 70R 215Y genotype is the predominant TAM pathway associated with virologic failure among HIV type 1C-infected adults treated with ZDV/ddI-containing HAART in southern Africa. AIDS Res. Hum. Retroviruses 23, 868–878.
Ntemgwa, M., Wainberg, M.A., Oliveira, M., Moisi, D., Lalonde, R., Micheli, V., Brenner, B.G., 2007. Variations in reverse transcriptase and RNase H domain mutations in human immunodeficiency virus type 1 clinical isolates are associated with divergent phenotypic resistance to zidovudine. Antimicrob. Agents Chemother. 51, 3861–3869.
Parkin, N.T., Hellmann, N.S., Whitcomb, J.M., Kiss, L., Chappey, C., Petropoulos, C.J., 2004. Natural variation of drug susceptibility in wild-type human immunodeficiency virus type 1. Antimicrob. Agents Chemother. 48, 437–443.
Rhee, S.Y., Taylor, J., Wadhera, G., Ben-Hur, A., Brutlag, D.L., Shafer, R.W., 2006. Genotypic predictors of human immunodeficiency virus type 1 drug resistance. Proc. Natl. Acad. Sci. USA 103, 17355–17360.
Romano, L., Venturi, G., Bloor, S., Harrigan, R., Larder, B.A., Major, J.C., Zazzi, M., 2002. Broad nucleoside-analogue resistance implications for human immunodeficiency virus type 1 reverse-transcriptase mutations at codons 44 and 118. J. Infect. Dis. 185, 898–904.
Roquebert, B., Marcelin, A.G., 2008. The involvement of HIV-1 RNase H in resistance to nucleoside analogues. J. Antimicrob. Chemother. 61, 973–975.
Roquebert, B., Wirden, M., Simon, A., Deval, J., Katlama, C., Calvez, V., Marcelin, A.G., 2007. Relationship between mutations in HIV-1 RNase H domain and nucleoside reverse transcriptase inhibitors resistance mutations in naive and pre-treated HIV infected patients. J. Med. Virol. 79, 207–211.
Santos, A.F., Lengruber, R.B., Soares, E.A., Jere, A., Sprinz, E., Martinez, A.M., Silveira, J., Sion, F.S., Pathak, V.K., Soares, M.A., 2008. Conservation patterns of HIV-1 RT connection and RNase H domains: Identification of new mutations in NRTI-treated patients. PLoS ONE 3, e1781.
Sarafianos, S.G., Das, K., Tantillo, C., Clark Jr., A.D., Ding, J., Whitcomb, J.M., Boyer, P.L., Hughes, S.H., Arnold, E., 2001. Crystal structure of HIV-1 reverse transcriptase in complex with a polypurine tract RNA:DNA. EMBO J. 20, 1449–1461.
Shimura, K., Kodama, E., Sakagami, Y., Matsuzaki, Y., Watanabe, W., Yamataka, K., Watanabe, Y., Ohata, Y., Doi, S., Sato, M., Kano, M., Ikeda, S., Matsuoka, M., 2008. Broad antiretroviral activity and resistance profile of the novel human immunodeficiency virus integrase inhibitor elvitegravir (JTK-303/GS-9137). J. Virol. 82, 764–774.
Ueno, T., Mitsuya, H., 1997. Comparative enzymatic study of HIV-1 reverse transcriptase resistant to 2′, 3′-dideoxynucleotide analogs using the single-nucleotide incorporation assay. Biochemistry 36, 1092–1099.
UK Collaborative Group on Monitoring the Transmission of HIV Drug Resistance, 2001. Analysis of prevalence of HIV-1 drug resistance in primary infections in the United Kingdom. BMJ 322, 1087–1088.
Weinstock, H.S., Zaidi, I., Heneine, W., Bennett, D., Garcia-Lerma, J.G., Douglas Jr., J.M., LaLota, M., Dickinson, G., Schwarcz, S., Torian, L., Wendell, D., Paul, S., Goza, G.A., Ruiz, J., Boyett, B., Kaplan, J.E., 2004. The epidemiology of antiretroviral drug resistance among drug-naive HIV-1-infected persons in 10 US cities. J. Infect. Dis. 189, 2174–2180.
Yap, S.H., Sheen, C.W., Fahey, J., Zanin, M., Tyssen, D., Lima, V.D., Wynhoven, B., Kuiper, M., Sluis-Cremer, N., Harrigan, P.R., Tachedjian, G., 2007. N348I in the connection domain of HIV-1 reverse transcriptase confers zidovudine and nevirapine resistance. PLoS Med. 4, e335.
Zelina, S., Sheen, C.W., Radzio, J., Mellors, J.W., Sluis-Cremer, N., 2008. Mechanisms by which the G333D mutation in human immunodeficiency virus type 1 reverse transcriptase facilitates dual resistance to zidovudine and lamivudine. Antimicrob. Agents Chemother. 52, 157–163.

Bioorganic & Medicinal Chemistry Letters 20 (2010) 1241–1246

Contents lists available at ScienceDirect

Bioorganic & Medicinal Chemistry Letters

journal homepage: www.elsevier.com/locate/bmcl

Synthesis and biological evaluation of novel allophenylnorstatine-based HIV-1 protease inhibitors incorporating high affinity P2-ligands

Arun K. Ghosh [a,*], Sandra Gemma [a], Elena Simoni [a], Abigail Baldridge [a], D. Eric Walters [b], Kazuhiko Ide [c], Yasushi Tojo [c], Yasuhiro Koh [c], Masayuki Amano [c], Hiroaki Mitsuya [c,d]

[a] Departments of Chemistry and Medicinal Chemistry, Purdue University, West Lafayette, IN 47907, United States
[b] Departments of Biochemistry and Molecular Biology, Rosalind Franklin University of Medicine and Science, North Chicago, IL 60064, United States
[c] Departments of Hematology and Infectious Diseases, Kumamoto University School of Medicine, Kumamoto 860-8556, Japan
[d] Experimental Retrovirology Section, HIV and AIDS Malignancy Branch, National Cancer Institute, Bethesda, MD 20892, United States

ARTICLE INFO

Article history:
Received 19 October 2009
Revised 20 November 2009
Accepted 23 November 2009
Available online 5 December 2009

Keywords:
HIV protease
Inhibitors
Darunavir
Allophenylnorstatine
Design
Synthesis

ABSTRACT

A series of stereochemically defined cyclic ethers as P2-ligands were incorporated in an allophenylnorstatine-based isostere to provide a new series of HIV-1 protease inhibitors. Inhibitors **3b** and **3c**, containing conformationally constrained cyclic ethers, displayed impressive enzymatic and antiviral properties and represent promising lead compounds for further optimization.

The introduction of protease inhibitors into highly active antiretroviral treatment (HAART) regimens with reverse transcriptase inhibitors represented a major breakthrough in AIDS chemotherapy.[1] This combination therapy has significantly increased life expectancy, and greatly improved the course of HIV management. Therapeutic inhibition of HIV-1 protease leads to morphologically immature and noninfectious viral particles.[2] However, under the selective pressure of chemotherapeutics, rapid adaptation of viral enzymes generates strains resistant to one or more antiviral agents.[3] As a consequence, a growing number of HIV/AIDS patients harbor multidrug-resistant HIV strains. There is ample evidence that such strains can be readily transmitted.[4] Therefore, one of the major current therapeutic objectives has been to develop novel protease inhibitors (PIs) with broad-spectrum activity against multidrug-resistant HIV-1 variants. In our continuing interest in developing concepts and strategies to combat drug-resistance, we have reported a series of novel PIs including Darunavir, TMC-126, GRL-06579, and GRL-02031.[5–8] These inhibitors have shown exceedingly potent enzyme inhibitory and antiviral activity as well as exceptional broad spectrum activity against highly cross-resistant mutants. Darunavir, which incorporates a (*R*)-(hydroxymethyl)-sulfonamide isostere and a stereochemically defined bis-tetrahydrofuran (bis-THF) as the P2-ligand, was initially approved for the treatment of patients with drug-resistant HIV and more recently, it has been approved for all HIV/AIDS patients including pediatrics[9] (Fig. 1).

Darunavir was designed based upon the 'backbone binding' concept developed in our laboratories. Darunavir-bound X-ray structure revealed extensive hydrogen bonding with the protease backbone throughout the enzyme active site.[10] The P2-bis-THF ligand is responsible for its superior drug-resistance properties. The bis-THF ligand has been documented as a privileged ligand for the S2-subsite. Incorporation of this ligand into other transition-state isosteres also resulted in significant potency enhancement.[11] Besides 3(*S*)-THF, and [3*aS*,5*S*,6*R*]-bis-THF, we have designed a number of other novel cyclic ether-based high affinity ligands. Incorporation of these ligands in (*R*)-(hydroxyethyl)-sulfonamide isosteres provided PIs with excellent potency and drug-resistance properties.[6–8] We then investigated the potential of these structure-based designed P2-ligands in a KNI-764-derived isostere designed by Mimoto and coworkers.[12] This PI incorporates an allophenylnorstatine isostere. Interestingly, KNI-764 has maintained good activity against HIV-1 clinical strains resistant to several FDA-approved PIs. The flexible *N*-(2-methyl benzyl) amide P2′-ligand may have been responsible for its activity against drug-resistant HIV-1 strains as the flexible chain allows better adaptability to mutations.[12,13] The bis-THF and other structure-based designed P2-ligands, make several critical

* Corresponding author. Tel.: +1 765 494 5323; fax: +1 765 496 1612.
E-mail address: akghosh@purdue.edu (A.K. Ghosh).

0960-894X/$ - see front matter © 2009 Elsevier Ltd. All rights reserved.
doi:10.1016/j.bmcl.2009.11.123

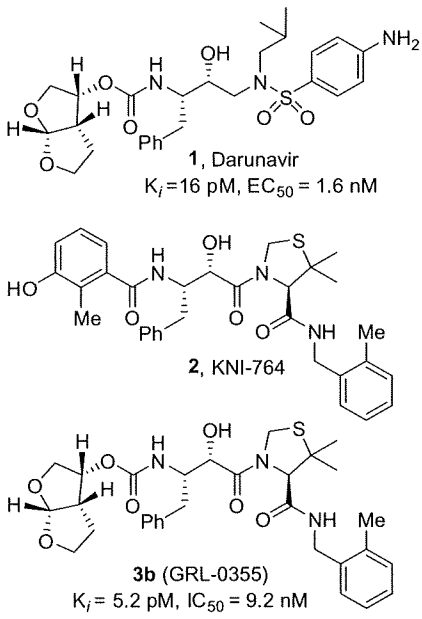

Figure 1. Structures of inhibitors **1**, **2**, and **3b**.

hydrogen bonds with the protein backbone, particularly with Asp-29 and Asp-30 NH's.[11] Therefore, incorporation of these ligands into the KNI-764-derived isostere, may lead to novel PIs with improved potency and efficacy against multidrug-resistant HIV-1 variants. Furthermore, substitution of the P2-phenolic derivative in KNI-764 with a cyclic ether-based ligand could result in improved metabolic stability and pharmacological properties since phenol glucuronide is readily formed when KNI-764 is exposed to human hepatocytes in vitro.[12]

The synthesis of target compounds **3a–e** was accomplished as described in Scheme 1. Our synthetic plan for carboxylic acid **7** (Scheme 1) involved the preparation of the key intermediate **5** through two different synthetic pathways. In the first approach, known optically active azidodiol **4**[14] was first hydrogenated in the presence of Boc_2O. The resulting diol was converted to **5** by selective acylation of the primary alcohol with acetic anhydride in the presence of pyridine and a catalytic amount of DMAP at 0 °C for 4 h to provide **5** in 77% overall yield. As an alternative approach, commercially available optically active epoxide **6** was exposed to lithium acetate, formed in situ from lithium carbonate and acetic acid in DMF. This resulted in the regioselective opening[15] of the epoxide ring and afforded compound **5** in 62% yield. The alcohol **5** thus obtained was protected as the corresponding acetonide by treatment with 2-methoxypropene in the presence of a catalytic amount of CSA. The acetate group was subsequently hydrolyzed in the presence of potassium carbonate in methanol to afford the corresponding alcohol. This was subjected to an oxidation reaction using ruthenium chloride hydrate and sodium periodate in a mixture of aqueous acetonitrile and CCl_4 at 23 °C for 10 h. This resulted in the formation of the target carboxylic acid **7** in 61% yield. Amide **9a** was prepared by activation of carboxylic acid **7** into the corresponding mixed anhydride by treatment with isobutylchloroformate followed by reaction with amine **8a.**[16,17]

Synthesis of various inhibitors was carried out as shown in Scheme 2. Deprotection of the Boc and acetonide groups was carried out by exposure of **9** to a 1 M solution of hydrochloric acid in methanol at 23 °C for 8 h. This provided amine **10** in quantitative

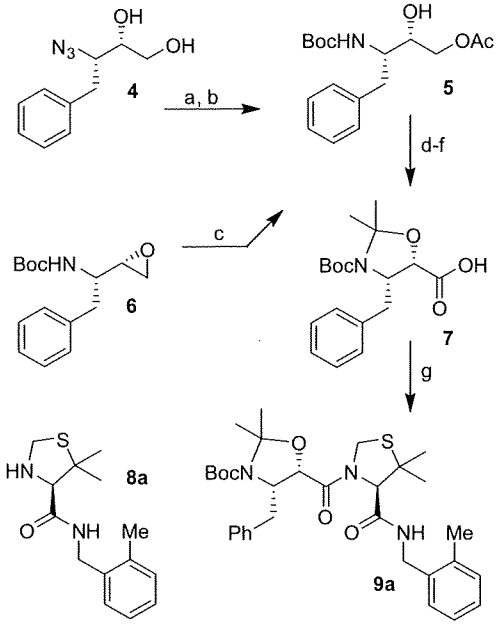

Scheme 1. Reagents: (a) H_2, Pd/C, Boc_2O, EtOAc; (b) Ac_2O, Pyr, DMAP; (c) $LiCO_3$, AcOH, DMF; (d) 2-methoxypropene, CSA, DCM; (e) K_2CO_3, MeOH; (f) $RuCl_3$, $NaIO_4$, CCl_4–MeCN–H_2O (2:2:3); (g) *N*-methylmorpholine, *i*BuOCOCl, **8a**, THF.

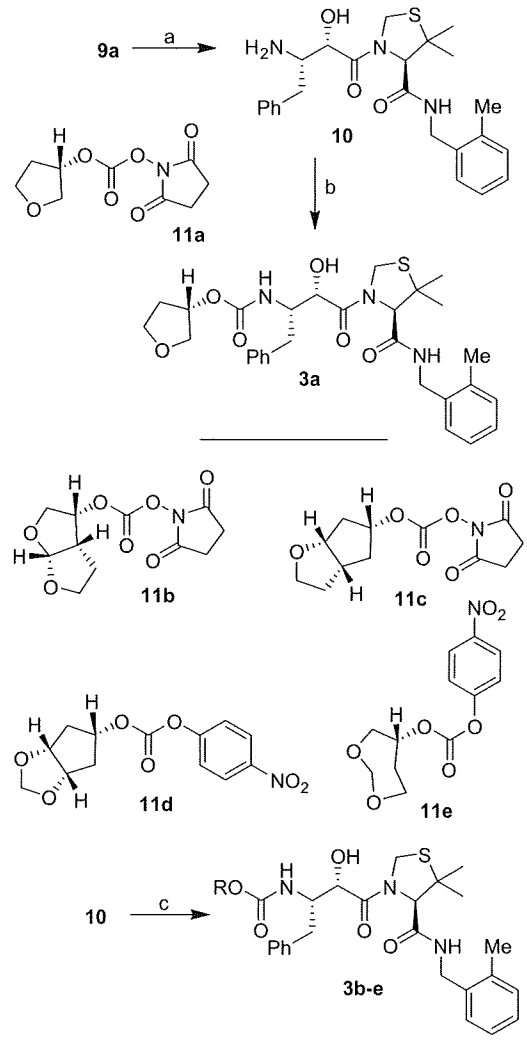

Scheme 2. Reagents: (a) 1 M HCl, MeOH; (b) **11a**, Et_3N, CH_2Cl_2; (c) **11b,c**, Et_3N, CH_2Cl_2; or, **11d,e**, DIPEA, THF.

yield. Reaction of **11a** with amine **10** in CH_2Cl_2 in the presence of Et_3N at 23 °C for 6 h, provided inhibitor **3a** in 62% yield. The 3(*S*)-tetrahydrofuranyl carbonate **11a** was prepared as described previously.[18] Similarly, allophenylnorstatine-based inhibitors **3b–e** were synthesized. As shown, carbonates **11b**,[19] **11c**,[7] and **11d–e**[19] were prepared as previously described. Reaction of these carbonates with amine **10** furnished the desired inhibitors **3b–e** in 45–62% yield.

The syntheses of inhibitors **14a,b** and **16a–c** were carried out as shown in Scheme 3. Inhibitors **14a,b**, containing hydroxyethylamine isostere were prepared by opening epoxide **6** with amine **8a** in the presence of lithium perchlorate in diethyl ether at 23 °C for 5 h to provide amino alcohol **12** in 64% yield. Removal of the Boc-group by exposure to 1 M HCl in MeOH at 23 °C for 12 h afforded amine **13**. Reactions of amine **13** with activated carbonates **11a** and **11b** afforded urethane **14a** and **14b** in 44% and 59% yields, respectively. For the synthesis of inhibitors **16a–c**, commercially available (*R*)-5,5-dimethyl-thiazolidine-4-carboxylic acid was protected as its Boc-derivative. The resulting acid was coupled with amines **15a–c** in the presence of DCC and DMAP in CH_2Cl_2 to provide the corresponding amides. Removal of the Boc-group by exposure to 30% trifluoroacetic acid afforded **8b–d**. Coupling of these amines with acid **7** as described in Scheme 1, provided the corresponding products **9b–d**. Removal of Boc-group and reactions of the resulting amines with activated carbonate **11b** furnished inhibitors **16a–c** in good yields (55–60%).

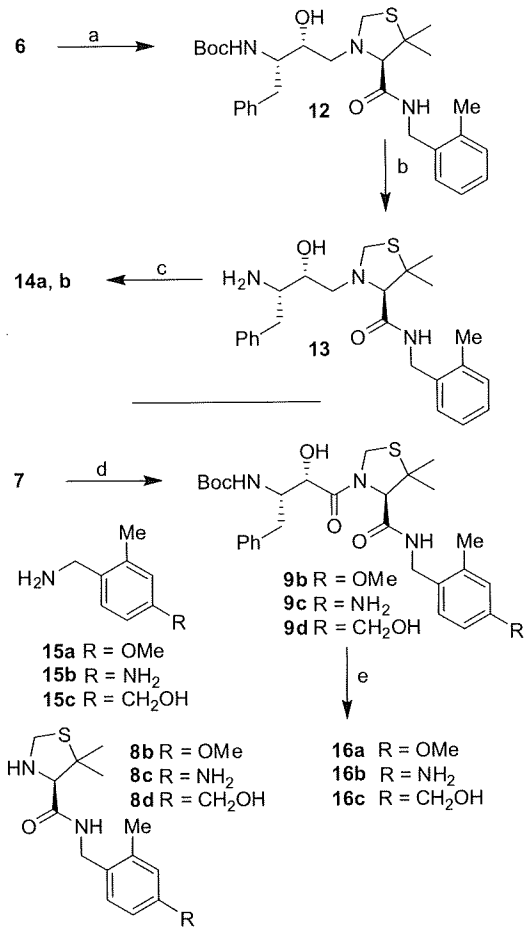

Scheme 3. Reagents: (a) **8a**, Li(ClO$_4$), Et_2O; (b) CF_3CO_2H, CH_2Cl_2; (c) **11a** or, **11b**, Et_3N, CH_2Cl_2; (d) *N*-methylmorpholine, *isobutylchloroformate*, **8b-d**, THF; (e) CF_3CO_2H, CH_2Cl_2, then **11b**, Et_3N, CH_2Cl_2.

Inhibitors **3a–e** were first evaluated in enzyme inhibitory assay utilizing the protocol described by Toth and Marshall.[20] Compounds that showed potent enzymatic K_i values were then further evaluated in antiviral assay. The inhibitor structure and potency are shown in Table 1. As shown, incorporation of a stereochemically defined 3(*S*)-tetrahydrofuran ring as the P2-ligand provided inhibitor **3a**, which displayed an enzyme inhibitory potency of 0.2 nM and antiviral IC_{50} value of 20 nM. The corresponding derivative **14a** with a hydroxyethylamine isostere exhibited over 400-fold reduction in enzyme inhibitory activity. Introduction of a stereochemically defined bis-THF as the P2-ligand, resulted in inhibitor **3b**, which displayed over 40-fold potency enhancement with respect to **3a**. Inhibitor **3b** displayed a K_i of 5.2 pM in the enzyme inhibitory assay. Furthermore, compound **3b** has shown an impressive antiviral activity with an IC_{50} value of 9 nM. Inhibitor **14b** with hydroxyethylamine isostere is significantly less potent than the corresponding norstatine-derived inhibitor **3b**. Inhibitor **3c** with a (3a*S*, 5*R*, 6a*R*)-5-hydroxy-hexahydrocyclopenta[*b*]furan as the P2-ligand has displayed excellent inhibitory activity, and particularly, antiviral activity, showing an IC_{50} value of 13 nM. Other structure-based designed ligands in inhibitors **3d** and **3e** have shown subnanomolar enzyme inhibitory activity. However, inhibitor **3b** with a bis-THF ligand has shown the most impressive activity.

To obtain molecular insight into the possible ligand-binding site interactions, we have created energy-minimized models of a number of inhibitors based upon protein-ligand X-ray structure of KNI-764 (**2**).[21] An overlayed model of **3b** with the X-ray structure of **2**-bound HIV-1 protease is shown in Figure 2. This model for inhibitor **3b** was created from the X-ray crystal structure of KNI-764 (**2**)-bound HIV-1 protease (KNI-764, pdb code 1MSM[21]) and the X-ray crystal structure of darunavir (pdb code 2IEN[22]), by combining the P2-end of the darunavir structure with the P2′-end of the KNI-764 structure, followed by 1000 cycles of energy minimization. It appears that both oxygens of the bis-THF ligand are suitably located to form hydrogen bonds with the backbone atoms of Asp-29 and Asp-30 NH's, similar to darunavir-bound HIV-1 protease.[10] Furthermore, the KNI-764-X-ray structure-derived model of **3b** suggested that the incorporation of appropriate substituents on the phenyl ring could interact with Asp-29′ and Asp-30′ in the S2′-subsite. In particular, it appears that a 4-hydroxymethyl substituent on the P2′-phenyl ring could conceivably interact with backbone Asp-30′ NH in the S2′-subsite. Other substituents such as a methoxy group or an amine functionality also appears to be within proximity to Asp-29′ and Asp-30′ backbone NHs. Based upon these speculations, we incorporated *p*-MeO, *p*-NH_2 and *p*-CH_2OH substituents on the P2′-phenyl ring of inhibitor **3b**. As shown in Table 1, neither *p*-MeO nor *p*-NH_2 groups improved enzyme inhibitory potency compared to inhibitor **3b**. Of particular note, compound **16a**, displayed a good antiviral potency, possibly suggesting a better penetration through the cell membrane. Inhibitor **16c** with a hydroxymethyl substituent showed sub-nanomolar enzyme inhibitory potency but its antiviral activity was moderate compared to unsubstituted derivative **3b**. As it turned out, inhibitor **3b** is the most potent inhibitor in the series. We subsequently examined its activity against a clinical wild-type X_4-HIV-1 isolate (HIV-$1_{ERS104pre}$) along with various multidrug-resistant clinical X_4- and R_5- HIV-1 isolates using PBMCs as target cells.[5b] As can be seen in Table 2, the potency of **3b** against HIV-$1_{ER104pre}$ (IC_{50} = 31 nM) was comparable to the FDA approved PI, amprenavir with an IC_{50} value of 45 nM. Darunavir and atazanavir on the other hand, are significantly more potent with IC_{50} values of 5 nM and 3 nM, respectively. Inhibitor **3b**, while less potent than darunavir, maintained 5-fold or better potency over amprenavir against HIV-$1_{MDR/C}$, HIV-$1_{MDR/G}$, HIV-$1_{MDR/TM}$ and HIV-$1_{MDR/MM}$. It maintained over a 2-fold potency against HIV-$1_{MDR/JSL}$. In fact, inhibitor **3b** maintained comparable potency to atazanavir against all

Table 1
Enzymatic inhibitory and antiviral activity of allophenylnorstatine-derived inhibitors

Entry	Inhibitor	K_i (nM)	IC_{50}[a,b] (μM)
1	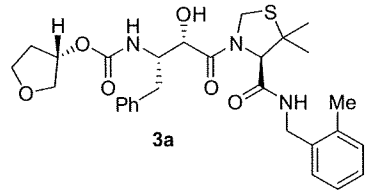 **3a**	0.21	0.02
2	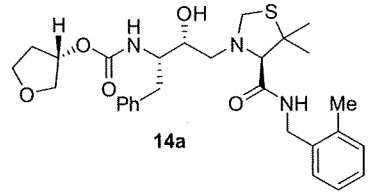 **14a**	86.2	nt
3	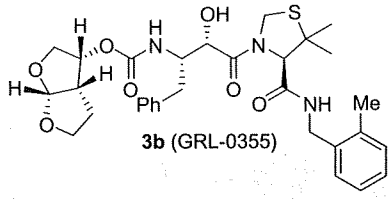 **3b** (GRL-0355)	0.0052	0.009
4	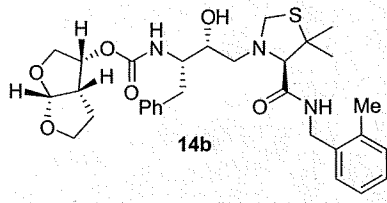 **14b**	2.6	nt
5	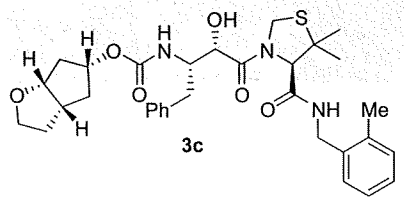 **3c**	0.29	0.013
6	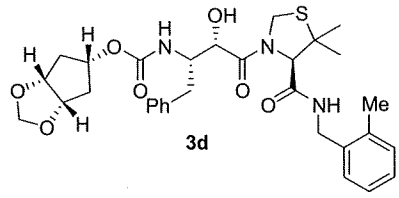 **3d**	0.65	nt
7	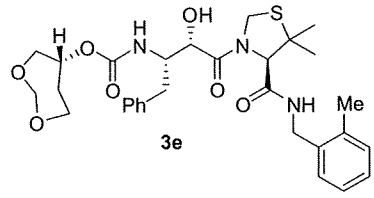 **3e**	0.78	nt
8	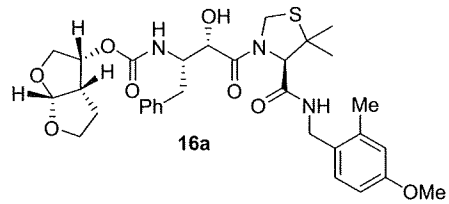 **16a**	2.03	0.051

Table 1 (*continued*)

Entry	Inhibitor	K_i (nM)	IC_{50}[a,b] (μM)
9	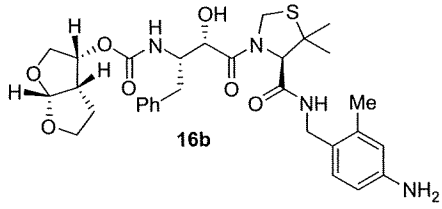 **16b**	1.01	0.53
10	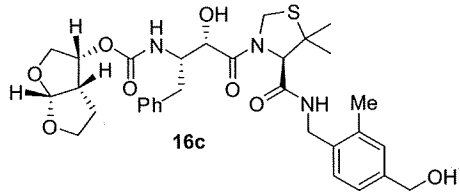 **16c**	0.31	0.23

[a] Values are means of at least three experiments.
[b] Human lymphoid (MT-2) cells were exposed to 100 $TCID_{50}$ values of HIV-1_{LAI} and cultured in the presence of each PI, and IC_{50} values were determined using MTT assay. Darunavir exhibited K_i = 16 pM, IC_{50} = 1.6 nM.

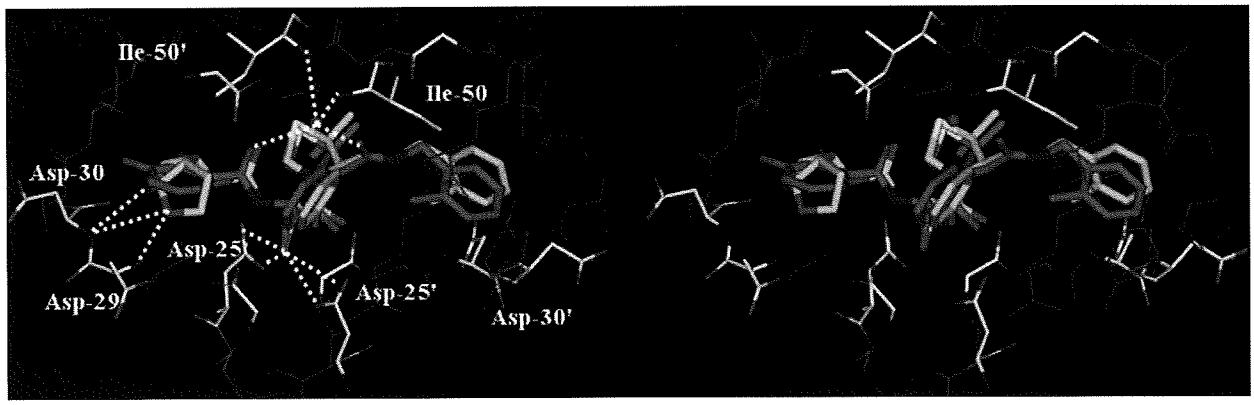

Figure 2. Structure of inhibitor **3b**, modeled into the active site of HIV-1 protease, superimposed on the X-ray crystal structure of KNI-764. Inhibitor **3b** carbons are shown in green and KNI-764 carbons are shown in magenta.

Table 2
Antiviral activity of **3b** (GRL-0355) against multidrug-resistant clinical isolates in PHA-PBMs.

Virus	IC_{50} (μM)			
	3b (GRL-0355)	APV	ATV	DRV
HIV-$1_{ERS104pre}$ (wild-type: X4)	0.031 ± 0.002	0.045 ± 0.014	0.003 ± 0.003	0.005 ± 0.001
HIV-$1_{MDR/C}$ (X4)	0.061 ± 0.005 (2)	0.346 ± 0.071 (8)	0.045 ± 0.026 (15)	0.010 ± 0.006 (2)
HIV-$1_{MDR/G}$ (X4)	0.029 ± 0.002 (1)	0.392 ± 0.037 (9)	0.029 ± 0.020 (10)	0.019 ± 0.005 (4)
HIV-$1_{MDR/TM}$ (X4)	0.064 ± 0.032 (2)	0.406 ± 0.082 (9)	0.047 ± 0.009 (16)	0.007 ± 0.003 (1)
HIV-$1_{MDR/MM}$ (R5)	0.042 ± 0.001 (1)	0.313 ± 0.022 (7)	0.040 ± 0.002 (13)	0.027 ± 0.008 (5)
HIV-$1_{MDR/JSL}$ (R5)	0.235 ± 0.032 (8)	0.531 ± 0.069 (12)	0.635 ± 0.065 (212)	0.028 ± 0.008 (6)

The amino acid substitutions identified in the protease-encoding region of HIV-$1_{ERS104pre}$, HIV-1_C, HIV-1_G, HIV-1_{MM}, HIV-1_{JSL} compared to the consensus type B sequence cited from the Los Alamos database include L63P; L10I, I15V, K20R, L24I, M36I, M46L, I54V, I62V, L63P, K70Q,V82A, L89M; L10I, V11I, T12E, I15V, L19I, R41K, M46L, L63P, A71T, V82A, L90M; L10I, K14R, R41K, M46L, I54V, L63P, A71V, V82A, L90M; L10I, K43T, M46L, I54V, L63P, A71V, V82A, L90M, Q92K; and L10I, L24I, I33F, E35D, M36I, N37S, M46L, I54V, R57K, I62V, L63P, A71V, G73S, V82A, respectively. HIV-$1_{ERS104pre}$ served as a source of wild-type HIV-1. The IC_{50} values were determined by using PHA-PBMs as target cells and the inhibition of p24 Gag protein production by each drug was used as an endpoint. The numbers in parentheses represent the fold changes of IC_{50} values for each isolate compared to the IC_{50} values for wild-type HIV-$1_{ERS104pre}$. All assays were conducted in duplicate, and the data shown represent mean values (±1 standard deviations) derived from the results of two or three independent experiments. Amprenavir = APV; Atazanavir = ATV; Darunavir = DRV.

multidrug-resistant clinical isolates tested. The reason for its impressive potency against multidrug-resistant clinical isolates is possibly due to its ability to make extensive hydrogen-bonds with the protease backbone in the S2 subsite and its ability to fill in the hydrophobic pockets in the S1′–S2′ subsites effectively.

In conclusion, incorporation of stereochemically defined and conformationally constrained cyclic ethers into the allophenylnorstatine resulted in a series of potent protease inhibitors. The promising inhibitors **3b** and **3c** are currently being subjected to further in-depth biological studies. Design and synthesis of new

classes of inhibitors based upon above molecular insight are currently ongoing in our laboratories.

Acknowledgement

The financial support of this work is provided by the National Institute of Health (GM 83356).

References and notes

1. Sepkowitz, K. A. *N. Eng. J. Med.* **2001**, *344*, 1764–1772.
2. Kohl, N. E.; Emini, E. A.; Schleif, W. A.; Davis, L. J.; Heimbach, J. C.; Dixon, R. A. F.; Scolnick, E. M.; Sigal, I. S. *Proc. Natl. Acad. Sci. U.S.A.* **1988**, *85*, 4686–4690.
3. (a) Pillay, D.; Bhaskaran, K.; Jurriaans, S.; Prins, M.; Masquelier, B.; Dabis, F.; Gifford, R.; Nielsen, C.; Pedersen, C.; Balotta, C.; Rezza, G.; Ortiz, M.; de Mendoza, C.; Kücherer, C.; Poggensee, G.; Gill, J.; Porter, K. *AIDS* **2006**, *20*, 21–28; (b) Grabar, S.; Pradier, C.; Le Corfec, E.; Lancar, R.; Allavena, C.; Bentata, M.; Berlureau, P.; Dupont, C.; Fabbro-Peray, P.; Poizot-Martin, I.; Costagliola, D. *AIDS* **2000**, *14*, 141–149.
4. Wainberg, M. A.; Friedland, G. *JAMA* **1998**, *279*, 1977–1983.
5. (a) Ghosh, A. K.; Kincaid, J. F.; Cho, W.; Walters, D. E.; Krishnan, K.; Hussain, K. A.; Koo, Y.; Cho, H.; Rudall, C.; Holland, L.; Buthod, J. *Bioorg. Med. Chem. Lett.* **1998**, *8*, 687–690; (b) Koh, Y.; Maeda, K.; Ogata, H.; Bilcer, G.; Devasamudram, T.; Kincaid, J. F.; Boross, P.; Wang, Y.-F.; Tie, Y.; Volarath, P.; Gaddis, L.; Louis, J. M.; Harrison, R. W.; Weber, I. T.; Ghosh, A. K.; Mitsuya, H. *Antimicrob. Agents Chemother.* **2003**, *47*, 3123–3129; (c) Ghosh, A. K.; Pretzer, E.; Cho, H.; Hussain, K. A.; Duzgunes, N. *Antiviral Res.* **2002**, *54*, 29–36.
6. Yoshimura, K.; Kato, R.; Kavlick, M. F.; Nguyen, A.; Maroun, V.; Maeda, K.; Hussain, K. A.; Ghosh, A. K.; Gulnik, S. V.; Erickson, J. W.; Mitsuya, H. *J. Virol.* **2002**, *76*, 1349–1358.
7. Ghosh, A. K.; Sridhar, P. R.; Leshchenko, S.; Hussain, A. K.; Li, J.; Kovalevsky, A. Y.; Walters, D. E.; Wedekind, J. K.; Grum-Tokars, V.; Das, D.; Koh, Y.; Maeda, K.; Gatanaga, H.; Weber, I. T.; Mitsuya, H. *J. Med. Chem.* **2006**, *49*, 5252.
8. Koh, Y.; Das, D.; Leshchenko, S.; Nakata, H.; Ogata-Aoki, H.; Amano, M.; Nakayama, M.; Ghosh, A. K.; Mitsuya, H. *Antimicrob. Agents Chemother.* **2009**, *53*, 997–1006.
9. (a) FDA approved Darunavir on June 23, 2006: FDA approved new HIV treatment for patients who do not respond to existing drugs. Please see: http://www.fda.gov/NewsEvents/Newsroom/PressAnnouncements/2006/ucm108676.htm (b) On October 21, 2008, FDA granted traditional approval to Prezista (darunavir), co-administered with ritonavir and with other antiretroviral agents, for the treatment of HIV-1 infection in treatment-experienced adult patients. In addition to the traditional approval, a new dosing regimen for treatment-naïve patients was approved.
10. Ghosh, A. K.; Chapsal, B. D.; Weber, I. T.; Mitsuya, H. *Acc. Chem. Res.* **2008**, *41*, 78–86.
11. Ghosh, A. K.; Ramu Sridhar, P.; Kumaragurubaran, N.; Koh, Y.; Weber, I. T.; Mitsuya, H. *ChemMedChem* **2006**, *1*, 939–950.
12. Mimoto, T.; Terashima, K.; Nojima, S.; Takaku, H.; Nakayama, M.; Shintani, M.; Yamaoka, T.; Hayashi, H. *Bioorg. Med. Chem.* **2004**, *12*, 281–293.
13. Yoshimura, K.; Kato, R.; Yusa, K.; Kavlick, M. F.; Maroun, V.; Nguyen, A.; Mimoto, T.; Ueno, T.; Shintani, M.; Falloon, J.; Masur, H.; Hayashi, H.; Erickson, J.; Mitsuya, H. *Proc. Natl. Acad. Sci. U.S.A.* **1999**, *96*, 8675–8680.
14. Ghosh, A. K.; Thompson, W. J.; Holloway, M. K.; McKee, S. P.; Duong, T. T.; Lee, H. Y.; Munson, P. M.; Smith, A. M.; Wai, J. M.; Darke, P. L.; Zugay, J.; Emini, E. A.; Schleif, W. A.; Huff, J. R.; Anderson, P. S. *J. Med. Chem.* **1993**, *36*, 2300–2310.
15. Ohmoto, K.; Okuma, M.; Yamamoto, T.; Kijima, H.; Sekioka, T.; Kitagawa, K.; Yamamoto, S.; Tanaka, K.; Kawabata, K.; Sakata, A., et al *Bioorg. Med. Chem. Lett.* **2001**, *9*, 1307–1323.
16. Ikunaka, M.; Matsumoto, J.; Nishimoto, Y. *Tetrahedron: Asymmetry* **2002**, *13*, 1201–1208.
17. Iwona Kudyba, I.; Raczko, J.; Jurczak, J. *J. Org. Chem.* **2004**, *69*, 2844–2850.
18. Ghosh, A. K.; Duong, T. T.; McKee, S. P. *Tetrahedron Lett.* **1992**, *33*, 2781–2784.
19. (a) Ghosh, A. K.; Leshchenko, S.; Noetzel, M. *J. Org. Chem.* **2004**, *69*, 7822–7829; (b) Ghosh, A. K.; Gemma, S.; Takayama, J.; Baldridge, A.; Leshchenko-Yashchuk, S.; Miller, H. B.; Wang, Y.-F.; Kovalevsky, A. Y.; Koh, Y.; Weber, I. T.; Mitsuya, H. *Org. Biomol. Chem.* **2008**, *6*, 3703–3713; (c) Ghosh, A. K.; Gemma, S.; Baldridge, A.; Wang, Y.-F.; Kovalevsky, A. Y.; Koh, Y.; Weber, I. T.; Mitsuya, H. *J. Med. Chem.* **2008**, *51*, 6021–6033.
20. Toth, M. V.; Marshall, G. R. A. *Int. J. Pep. Protein Res.* **1990**, *36*, 544–550.
21. Vega, S.; Kang, L.-W.; Velazquez-Campoy, A.; Kiso, Y.; Amzel, L. M.; Freire, E. *Proteins* **2004**, *55*, 594–602.
22. Kovalevski, A. Y.; Louis, J. M.; Aniana, A.; Ghosh, A. K.; Weber, I. T. *J. Mol. Biol.* **2008**, *384*, 178–192.

Design of HIV-1 Protease Inhibitors with Pyrrolidinones and Oxazolidinones as Novel P1′-Ligands To Enhance Backbone-Binding Interactions with Protease: Synthesis, Biological Evaluation, and Protein−Ligand X-ray Studies[∞]

Arun K. Ghosh,*[,†] Sofiya Leshchenko-Yashchuk,[†] David D. Anderson,[†] Abigail Baldridge,[†] Marcus Noetzel,[†] Heather B. Miller,[†] Yunfeng Tie,[‡] Yuan-Fang Wang,[‡] Yasuhiro Koh,[⊥] Irene T. Weber,[‡] and Hiroaki Mitsuya[||,⊥]

Departments of Chemistry and Medicinal Chemistry, Purdue University, West Lafayette, Indiana 47907, Department of Biology, Molecular Basis of Disease, Georgia State University, Atlanta, Georgia 30303, Departments of Hematology and Infectious Diseases, Kumamoto University School of Medicine, Kumamoto 860-8556, Japan, and Experimental Retrovirology Section, HIV and AIDS Malignancy Branch, National Cancer Institute, Bethesda, Maryland 20892

Received March 10, 2009

Structure-based design, synthesis, and biological evaluation of a series of novel HIV-1 protease inhibitors are described. In an effort to enhance interactions with protease backbone atoms, we have incorporated stereochemically defined methyl-2-pyrrolidinone and methyl oxazolidinone as the P1′-ligands. These ligands are designed to interact with Gly-27′ carbonyl and Arg-8 side chain in the S1′-subsite of the HIV protease. We have investigated the potential of these ligands in combination with our previously developed bis-tetrahydrofuran (bis-THF) and cyclopentanyltetrahydrofuran (Cp-THF) as the P2-ligands. Inhibitor **19b** with a (*R*)-aminomethyl-2-pyrrolidinone and a Cp-THF was shown to be the most potent compound. This inhibitor maintained near full potency against multi-PI-resistant clinical HIV-1 variants. A high resolution protein−ligand X-ray crystal structure of **19b**-bound HIV-1 protease revealed that the P1′-pyrrolidinone heterocycle and the P2-Cp-ligand are involved in several critical interactions with the backbone atoms in the S1′ and S2 subsites of HIV-1 protease.

Introduction

Advances in the treatment of HIV[a]/AIDS with HIV-1 protease inhibitors in combination with reverse transcriptase inhibitors have been widely documented.[1] The combination therapy, also known as highly active antiretroviral therapy (HAART), blocks critical viral replication at two different stages of the replication cycle.[2] The HAART regimens have resulted in dramatic reduction of blood plasma viral load levels, increased CD_4^+ lymphocyte counts, and improved life expectancy and significantly reduced HIV/AIDS-related mortality in the developed world.[3] Despite these important advances, effective long-term suppression of HIV infection with HAART regimens is a complex issue in medicine for a number of reasons. These include drug side effects, poor penetration into protected HIV reservoir sites, poor oral bioavailability, and interactions between drugs.[4] Perhaps one of the most daunting problems in future management of HIV is the emergence of drug-resistant HIV-1 variants and the transmission of these viral strains.[5,6] Thus, development of antiretroviral therapy with broad-spectrum activity and minimal drug side effects is critical for an effective management of current and future HIV/AIDS treatment. We recently reported the design and development of a number of exceedingly potent nonpeptidic HIV-1 protease inhibitors (PIs) **1**−**3** (Figure 1).[7−9] One of those PIs is darunavir (**1**, TMC-114), which was approved by the FDA in 2006 for the treatment of HIV/AIDS patients who are harboring drug-resistant HIV and do not respond to other therapies.[10] More recently, darunavir has received full approval for all HIV/AIDS patients.[11]

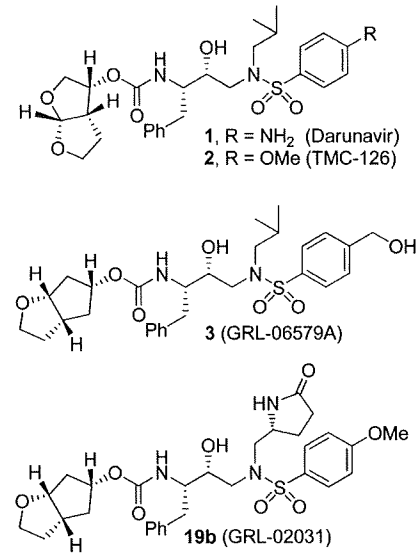

Figure 1. Structures of inhibitors **1**−**3** and **19b**.

To combat drug resistance, our structure-based design strategies are to maximize the protease active-site interactions with the inhibitor and particularly to promote extensive hydrogen bonding with the protein backbone atoms.[12] It is evident that active site backbone conformation of mutant proteases is only minimally distorted compared to that of the wild-type HIV-1 protease.[13,14] Therefore, the "backbone binding" strategy may be important to combat drug resistance.[12] Using high resolution protein−ligand X-ray structures of **1**- and **3**-bound HIV-1

[∞] The PDB accession code for **19b**-bound HIV-1 protease X-ray structure is 3H5B.

* To whom correspondence should be addressed. Phone: (765) 494-5323. Fax: (765) 496-1612. E-mail: akghosh@purdue.edu.

[†] Purdue University.

[‡] Georgia State University.

[⊥] Kumamoto University School of Medicine.

[||] National Cancer Institute.

[a] Abbreviations: HIV, human immunodeficiency virus; bis-THF, bis-tetrahydrofuran; Cp-THF, cyclopentanyltetrahydrofuran; PI, protease inhibitor; HAART, highly active antiretroviral therapy; APV, amprenavir; DRV, darunavir; SQV, saquinavir; IDV, indinavir; LPV, lopinavir; RTV, ritonavir.

10.1021/jm900303m CCC: $40.75
Published on Web 05/27/2009

Scheme 1. Synthesis of Lactam Containing Sulfonamide Isosteres

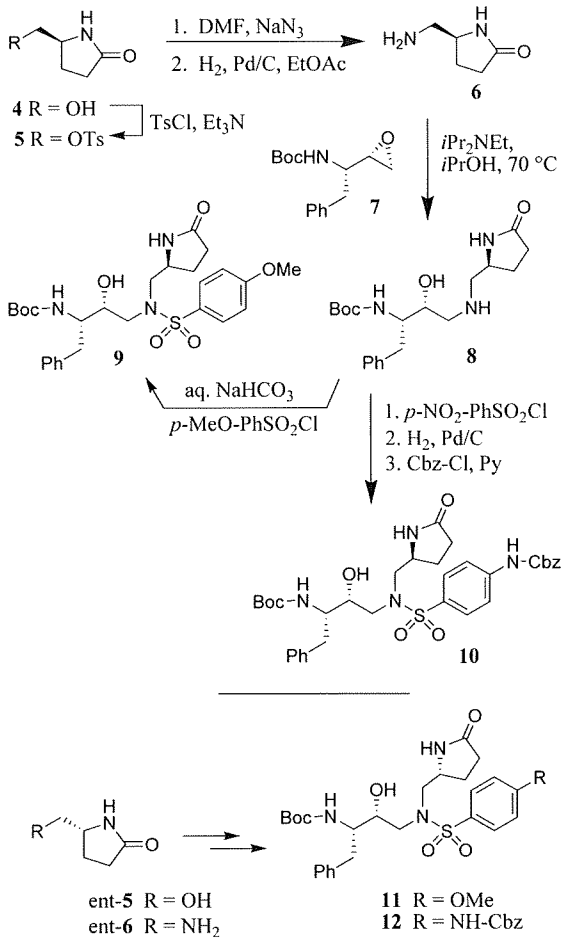

Scheme 2. Synthesis of Lactam Containing PIs

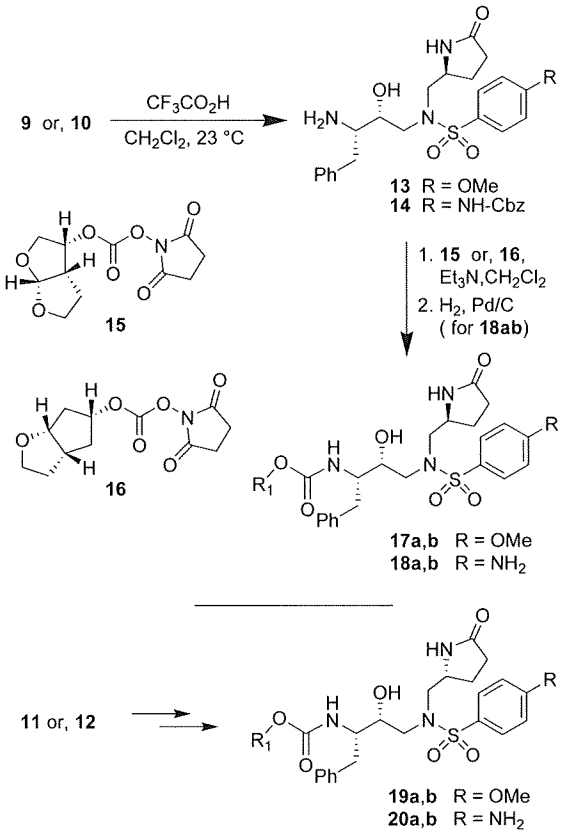

protease, we have shown that these PIs were engaged in extensive hydrogen bonding interactions with the backbone atoms throughout the active site cavity from the S2 to S2′ regions.[9,15] To further enhance "backbone binding" interactions, we became interested in designing an appropriately functionalized P1′-ligand that could interact with the backbone atoms, particularly with the Gly-27′ and Arg-8 in the S1′-subsite. This enhancement of "backbone binding" interaction may lead to inhibitors with improved drug-resistance profiles. Herein, we report the design, synthesis, and biological evaluation of a series of potent HIV-1 protease inhibitors that incorporated structure-based designed stereochemically defined lactam and oxazolidinone derivatives as the P1′-ligands in combination with the bis-THF or Cp-THF as the P2-ligands. Inhibitor **19b** incorporating a (*R*)-5-aminomethyl-2-pyrrolidinone as the P1′-ligand and Cp-THF as the P2-ligand is the most potent PI in the series. Interestingly, this PI has retained full potency against a range of multidrug-resistant HIV-1 variants. The protein−ligand X-ray structure of **19b**-bound HIV-1 protease revealed important molecular insight into the ligand-binding site interactions.

Chemistry

The optically active synthesis of the requisite 5-aminomethyl-2-pyrrolidinone for P1-ligands and their conversion to respective sulfonamide isostere are shown in Scheme 1. Commercially available 5-(*S*)-hydroxymethyl-2-pyrrolidinone **4** was reacted with tosyl chloride and triethylamine to provide tosylate **5**. Displacement of the tosylate with sodium azide in DMF at 55 °C for 9 h provided the azide derivative in 92% yield over two steps. Catalytic hydrogenation of the azide over 10% Pd−C in ethyl acetate afforded optically active amine **6** in quantitative yield. 5-(*R*)-Hydroxymethyl-2-pyrrolidinone (*ent*-**5**) was similarly converted to optically active amine *ent*-**6** in comparable yield. Amine **6** was reacted with commercially available epoxide **7** in the presence of *i*-Pr_2NEt (DIPEA) in 2-propanol at 70 °C for 36 h to provide epoxide-opened product **8** in 85% yield.[16] Amine **8** was converted to *p*-methoxybenezenesulfonamide derivative **9** by reaction with *p*-methoxybenzenesulfonyl chloride in the presence of aqueous $NaHCO_3$ in quantitative yield. Treatment of amine **8** with *p*-nitrobenzenesulfonyl chloride afforded the corresponding nitrosulfonamide. Catalytic hydrogenation over 10% Pd−C gave the corresponding aniline derivative, which was reacted with benzyl chloroformate in the presence of pyridine to furnish Cbz-derivative **10** in 63% yield for three steps. Enantiomeric amine (*ent*-**6**) was converted to the respective methoxy and Cbz-derived **11** and **12** by analogous procedures.

The synthesis of various PIs incorporating methylpyrrolidinones as the P1′-ligand is shown in Scheme 2. Exposure of Boc-derivatives **9** and **10** to 30% CF_3CO_2H in CH_2Cl_2 at 23 °C for 40 min resulted in the respective amines **13** and **14**. Alkoxycarbonylation of amine **13** with activated mixed carbonates **15**[16] and **16**[9] in the presence of Et_3N in CH_2Cl_2 furnished inhibitors **17a** and **17b** in 98% and 87% yields, respectively.[17] Alkoxycarbonylation of amine **14** with activated carbonates **15** and **16** afforded the corresponding Cbz-protected urethanes. Removal of the Cbz-group by catalytic hydrogenation over 10% Pd−C in ethyl acetate provided inhibitor **18a** and **18b** in 58% and 62% yields, respectively. Sulfonamide derivatives **11** and **12** containing enantiomeric P1′-ligands were converted to inhibitors **19a,b** and **20a,b** by following analogous procedures.

The synthesis of sulfonamide isosteres incorporating methyloxazolidinone as the P1′-ligand is shown in Scheme 3. Optically

Scheme 3. Synthesis of Sulfonamide Isosteres with P_1'-Oxazolidinone

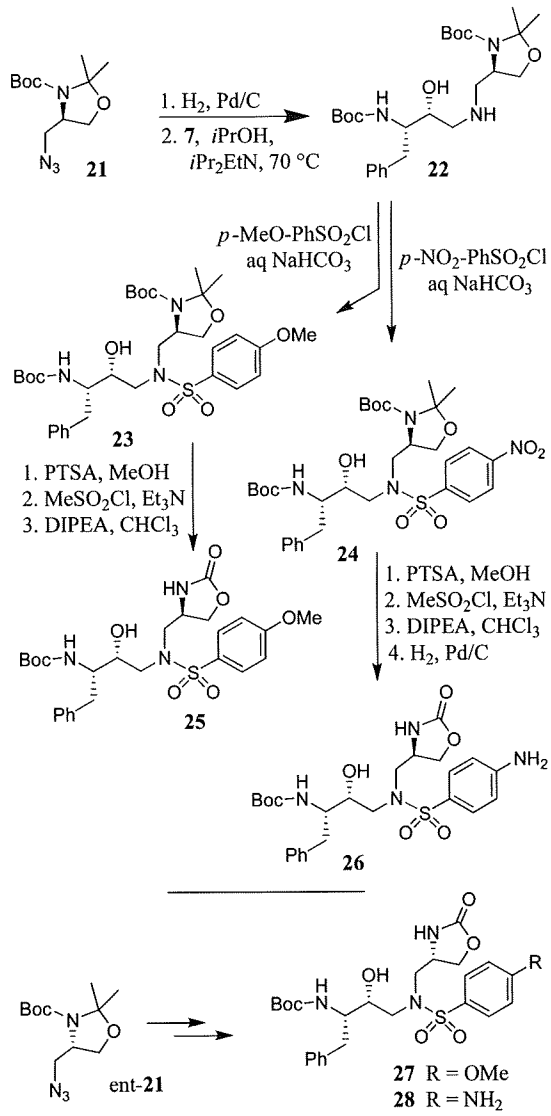

active dimethyloxazolidines **21** and *ent*-**21** were prepared by following the procedure described by Dondini and co-workers.[18] Reduction of these azides by catalytic hydrogenation in methanol afforded the respective amine. Reaction of **21**-derived amine with epoxide **7** in the presence of *i*-Pr_2NEt in 2-propanol afforded amine **22** in 41% yield. Reaction of amine **22** with *p*-methoxybenzenesulfonyl chloride or *p*-nitrobenzenesulfonyl chloride as described previously afforded sulfonamide derivatives **23** and **24** in 80% and 92% yields, respectively. The isopropylidene functionality in **23** and **24** was converted to the corresponding oxazolidinone derivative in a three-step sequence involving (1) treatment of **23** by a catalytic amount of *p*-toluenesulfonic acid (PTSA) in methanol, resulting in the removal of the isopropylidene group, (2) reaction of the resulting Boc-amino alcohol with mesyl chloride in the presence of triethylamine to provide the corresponding mesylate, and (3) treatment of the resulting mesylate with *i*-Pr_2NEt in chloroform at reflux. This has provided oxazolidinone **25** in 45% yield over three steps. The nitrosulfonamide derivative **24** was similarly converted to the corresponding oxazolidinone. Catalytic hydrogenation of the resulting nitro derivative with 10% Pd–C in methanol provided aniline derivative **26** in 37% overall yield

Scheme 4. Synthesis of Oxazolidinone-Derived PIs

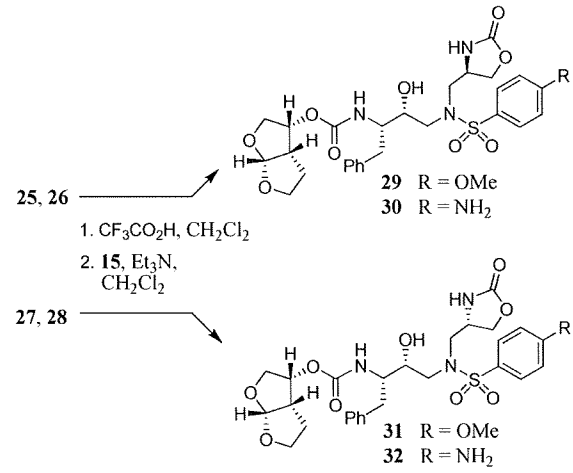

over four steps. Enantiomeric azide *ent*-**21** was converted to oxazolidinone derivatives **27** and **28** by following analogous procedures.

The synthesis of inhibitors containing oxazolidinone as P1′-ligand and bis-THF as the P2-ligand is shown in Scheme 4. Treatment of oxazolidinones **25**–**28** with 30% CF_3CO_2H in CH_2Cl_2 at 23 °C afforded the corresponding amines. Reaction of the resulting amines with activated mixed carbonate **15** in the presence of Et_3N in CH_2Cl_2 afforded the target inhibitors **29**–**32** in excellent yields (80–90%). The structures of these inhibitors are shown in Table 1.

Results and Discussion

Our examination of the X-ray structure of **1**-bound HIV-1 protease and its respective modeling initially suggested that a methyl-2-pyrrolidinone may interact well with residues in the S1′-site.[15] As shown in Table 1, our first set of inhibitors contain a (*R*)-hydroxyethylamine sulfonamide isostere with either the bis-THF or Cp-THF as the P2-ligand and *p*-methoxysulfonamide or *p*-aminosulfonamide as the P2′-ligand. The enzyme inhibitory potency of these PIs was evaluated according to the procedure reported by Toth and Marshall.[19] Inhibitor **17a** with (*S*)-methyl-2-pyrrolidinone displayed an enzyme K_i of 1 nM. Inhibitor **17b** with a Cp-THF showed a 3-fold improvement of potency. Antiviral activity of these inhibitors was determined in MT-2 human T-lymphoid cells exposed to $HIV\text{-}1_{LAI}$. Interestingly, both inhibitors have shown dramatic reduction in antiviral activity. Inhibitors **17a** and **17b** have shown IC_{50} values of 0.48 and 0.23 μM, respectively. However, these inhibitors are significantly less potent compared to inhibitors with an isobutyl group as the P1′-ligand.[7c,9] Incorporation of *p*-aminosulfonamide (PIs **18a** and **18b**) as the P2′-ligand led to a drop in enzyme inhibitory as well as antiviral potency. Inhibitor **19a** containing (*R*)-methyl-2-pyrrolidinone as the P1′-ligand has shown 10-fold enhancement of enzyme K_i over the (*S*)-isomer **17a**. It showed a slight improvement in antiviral activity compared to inhibitor **17a**. Inhibitor **19b** with (*R*)-methyl-2-pyrrolidinone as the P1′-ligand and Cp-THF as the P2-ligand resulted in the most potent inhibitor in the series. It has shown an enzymatic K_i of 99 pM and a 10-fold improvement (IC_{50} = 0.026 μM) in antiviral activity relative to epimeric (*S*)-pyrrolidinone derivative **17b**, suggesting an important role for the P1′-ring stereochemistry. Indeed, an X-ray structure of **19b**-bound HIV-1 protease revealed that the pyrrolidinone carbonyl and the NH functionalities were positioned to hydrogen-bond with residues in the S1′-site. Interestingly, the combination of P1′-methylpyrrolidi-

Table 1. Enzymatic Inhibitory Activity of Lactam and Oxazolidinone Containing Inhibitors[b]

Entry	Inhibitor	K_i (nM)	IC_{50}(nM)[a]
1.	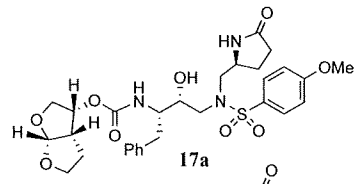 **17a**	0.85±0.02	0.48±0.05
2.	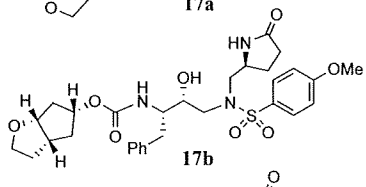 **17b**	0.31±0.03	0.23±0.08
3.	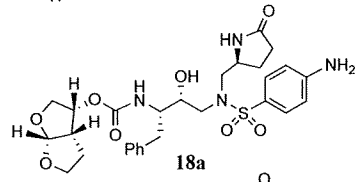 **18a**	0.28±0.03	>1
4.	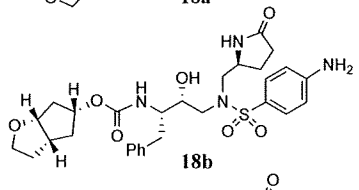 **18b**	1.27±0.15	>1
5.	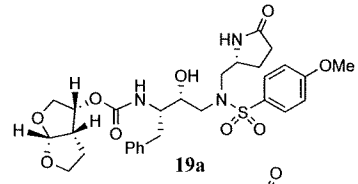 **19a**	0.12±0.003	0.25±0.11
6.	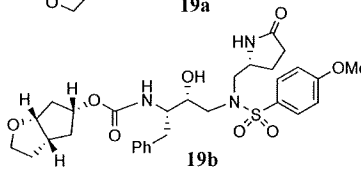 **19b**	0.099±0.003	0.026±0.002
7.	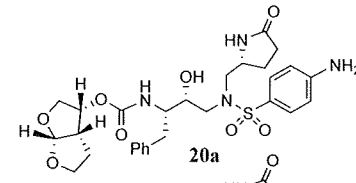 **20a**	0.85±0.2	>1
8.	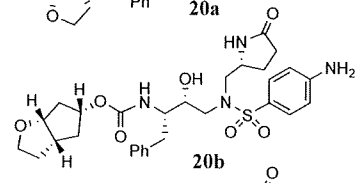 **20b**	0.31±0.03	0.60±0.24
9.	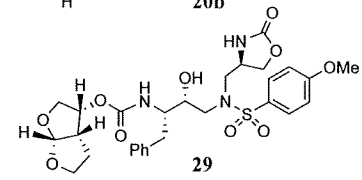 **29**	0.28±0.03	0.48±0.17
10.	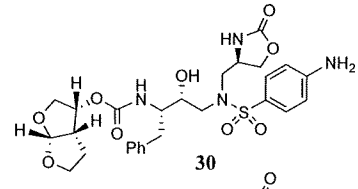 **30**	0.31±0.03	>1
11.	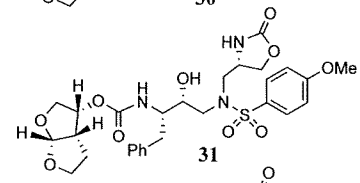 **31**	0.035±0.01	0.31±0.21
12.	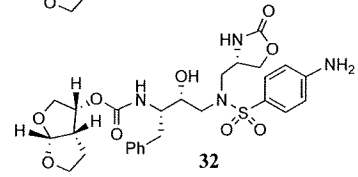 **32**	0.24±0.03	>1

[a] Values are the mean of at least two experiments. [b] Human T-lymphoid (MT-2) cells (2×10^3) were exposed to 100 $TCID_{50}$ values of HIV-1_{LAI} and cultured in the presence of each PI, and IC_{50} values were determined using the MTT assay. The IC_{50} values of amprenavir (APV), saquinavir (SQV), and indinavir (IDV) were 0.03, 0.015, and 0.03 μM, respectively.

none and polar P2′-*p*-aminosulfonamide led to PIs with subnanomolar enzyme activity. However, antiviral activity was reduced drastically. In PIs **29**−**32**, we have incorporated both (*S*)- and (*R*)-oxazolidinone derivatives as substitutes for the respective pyrrolidinone isomers. As can be seen, oxazolidinone derivatives **29**−**32** have shown subnanomolar enzyme inhibitory potency. Inhibitors with *p*-methoxysulfonamide as the P2′-ligand displayed comparable antiviral activity relative to pyrrolidinone derivatives. Consistent with stereochemical preference, the (*R*)-oxazolidinone with *p*-methoxysulfonamide has shown better enzyme K_i values. However, the antiviral activity of these compounds is very similar. In general, both pyrrolidinone and oxazolidinone functionalities appear to be nicely accommodated in the S1′-site.

While inhibitor **31** is very potent in enzyme inhibitory assay, the significant reduction of antiviral potency is possibly due to poor cellular permeability of this polar functionality. Inhibitor **19b** appeared to be most potent among the series of inhibitors examined. It exhibited comparable antiviral activity with the FDA approved PIs amprenavir, saquinavir, and indinavir in the same assay.

Inhibitor **19b** was subsequently examined for its activity against a clinical wild-type X_4-HIV-1 isolate (HIV-$1_{ERS104pre}$) along with various multidrug-resistant clinical X_4- and R_5-HIV-1 isolates using PBMCs as target cells.[8b] As can be seen in Table 2, the potency of **19b** against HIV-$1_{ER104pre}$ (IC_{50} = 28 nM) was comparable to FDA approved PIs indinavir, amprenavir, and lopinavir with IC_{50} values of 28, 25, and 30 nM, respectively. Darunavir, on the other hand, is nearly 10-fold more potent (IC_{50} = 3.6 nM) than **19b** and the above-mentioned PIs. Interestingly, of all the PIs tested, indinavir was least able to suppress the replication of the multidrug-resistant clinical isolate examined (HIV-$1_{MDR/MM}$, HIV-$1_{MDR/TM}$, HIV-$1_{MDR/C}$, and HIV-$1_{MDR/G}$) with IC_{50} values greater than 1 μM. Both amprenavir and lopinavir displayed 10-fold or greater reduction in potency except against HIV-1MDR/G, where lopinavir showed a 5-fold reduction in potency. A more detailed virologic study using inhibitor **19b** will be published elsewhere.[20] Darunavir has maintained impressive activity against all the multidrug-resistant variants. Inhibitor **19b**, while less potent than darunavir, maintained near full potency against multidrug-resistant clinical isolates examined. This impressive drug-resistance property of **19b** is possibly due to its extensive interactions, particularly its ability to make extensive hydrogen bonding throughout the active site of the protease's backbone. Furthermore, inhibitor **19b** blocked the infection and replication

Table 2. Anti-HIV Activity of **19b** against Selected Clinical Isolates Highly Resistant to Multiple Protease Inhibitors[a]

		EC_{50} (μM)				
virus	phenotype	IDV	APV	LPV	DRV	**19b**
HIV-$1_{ERS104pre}$ (wild-type)	X4	0.028 ± 0.005	0.025 ± 0.006	0.03 ± 0.001	0.0036 ± 0.0002	0.028 ± 0.004
HIV-1_{TM} (MDR)	X4	>1 (>36)	0.25 ± 0.02 (10)	0.73 ± 0.53 (24)	0.0036 ± 0.0002 (1)	0.029 ± 0.004 (1)
HIV-1_{MM} (MDR)	R5	>1 (>36)	0.32 ± 0.03 (13)	0.72 ± 0.31 (24)	0.019 ± 0.009 (5)	0.042 ± 0.002 (2)
HIV-1_{C} (MDR)	X4	>1 (>36)	0.35 ± 0.03 (14)	0.32 ± 0.01 (11)	0.015 ± 0.001 (4)	0.023 ± 0.007 (1)
HIV-1_{G} (MDR)	X4	0.29 ± 0.07 (10)	0.33 ± 0.16 (13)	0.14 ± 0.01 (5)	0.014 ± 0.006 (4)	0.027 ± 0.001 (1)

[a] Amino acid substitutions identified in the protease-encoding regions of HIV-$1_{ERS104pre}$, HIV-1_{TM}, HIV-1_{MM}, HIV-1_{C}, and HIV-1_{G} compared to the consensus B sequence cited from the Los Alamos data base include L63P, L10I/K14R/R41K/M46L/I54V/L63P/A71V/V82A/L90M/I93L, L10I/K43T/M46L/I54V/L63P/A71V/V82A/L90M/Q92K, L10I/I15V/K20R/L24I/M36I/M46L/I54V/I62V/L63P/K70Q/V82A/L89M, and L10I/V11I/T12E/I15V/L19I/R41K/M46L/L63P/A71T/V82A/L90M, respectively. The EC_{50} values were determined by employing PHA-PBM as target cells and the inhibition of p24 *Gag* protein production as an end point. All values were determined in duplicate or triplicate, and those shown are derived from the results of three independent experiments. Numbers in parentheses represent fold changes of EC_{50} values against each isolate compared to EC_{50} values against HIV-$1_{ERS104pre}$. MDR: multidrug-resistant.

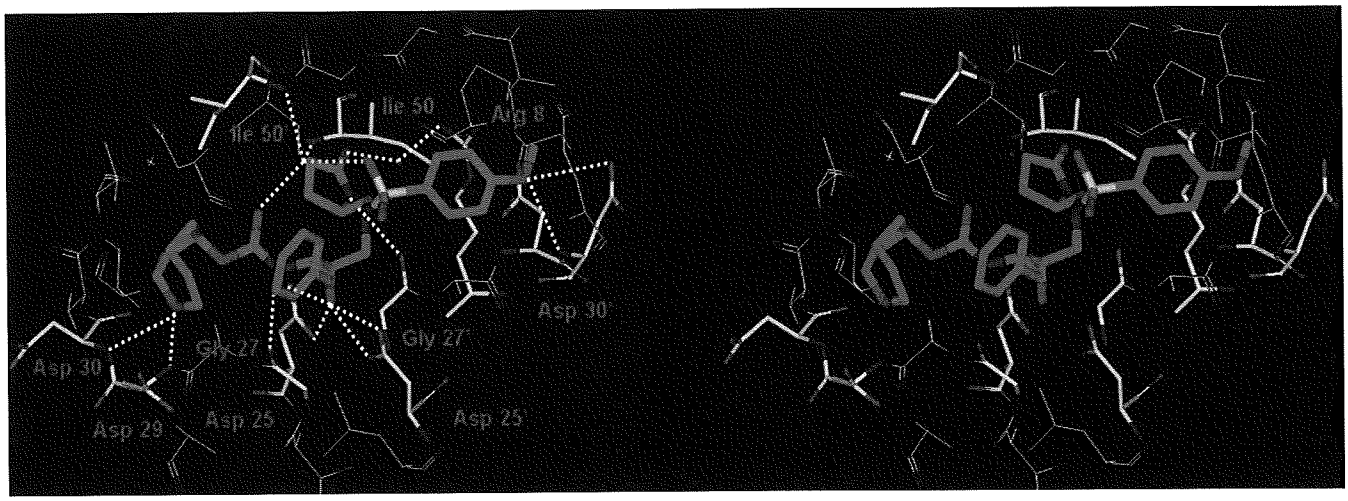

Figure 2. Stereoview of the major conformation of the X-ray structure of inhibitor **19b**-bound HIV-1 protease.

of each of the HIV-1_{NL4-3} variants exposed to and selected by up to 5 μM saquinavir, amprenavir, indinavir, nelfinavir, or ritonavir and a 1 μM lopinavir or atazanavir with EC_{50} values ranging from 0.036 to 0.14 μM.[20]

X-ray Crystallography. The binding mode of inhibitor **19b** was determined from the X-ray crystal structure of its complex with wild-type HIV-1 protease. The crystal structure was solved and refined at 1.29 Å resolution with an *R* factor of 14.1%. In this high resolution structure, the inhibitor was bound to the HIV-1 protease active site in two orientations with the relative occupancy of 0.8/0.2. The protease dimer comprises residues 1−99 and 1′−99′ of the two subunits, and the inhibitor binding site is formed by both subunits. The P1′-pyrrolidine ring also showed two alternative conformations with equal occupancy and related by about 18° rotation around the C12−C13 bond. A stereoview of the major conformation is shown in Figure 2 (only one conformation is shown for P1′). As shown, extensive interactions from P2 to P2′ were observed between the inhibitor and the protease active site, most notably favorable polar interactions including hydrogen bonds, weaker C−H···O and C−H···π interactions. The isostere hydroxyl group forms asymmetric hydrogen bonds to the carboxylate oxygen atoms of the catalytic Asp25 and Asp25′ with distances of 2.4−3.3 Å. Also, four direct hydrogen bonds are formed between the oxygens or nitrogens of the inhibitor atoms and the protease backbone atoms. These include cyclic ether oxygen of the P2-Cp-THF and the Asp-29 NH, the urethane NH with the carbonyl oxygen of Gly-27, P2′-methoxy oxygen and Asp-30′ NH. One conformation of the P1′-pyrrolidinone formed a hydrogen bond between the NH and the carbonyl oxygen of Gly-27′ and a water-mediated hydrogen bond between the P1′-pyrrolidinone

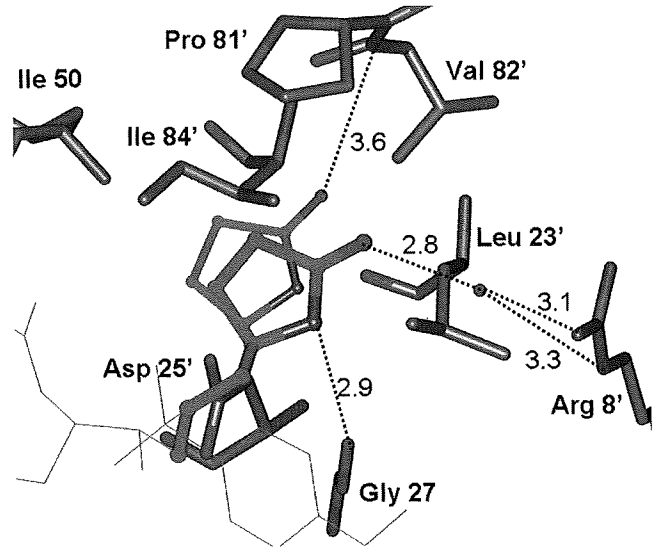

Figure 3. Protease interactions with the two alternate conformations of the inhibitor's pyrrolidine ring. The inhibitor is in green with thick bonds for the major and thin bonds for the minor conformations of the pyrrolidine ring. Hydrogen bonds are shown as dotted lines. Distances between donor and acceptor atoms are shown in Å.

carbonyl and the side chain of Arg-8. The other conformation of the P1′ group formed hydrophobic and C−H···O interactions with Pro-81′ and Val-82′, as shown in Figure 3. Also, there exists a tetracoordinated water-mediated interaction where the amides of Ile50 and Ile50′ donate hydrogen bonds, and the inhibitor's urethane carbonyl and one of the sulfonamide oxygen